

IMPROVED MOCK GALAXY CATALOGS FOR THE DEEP2 GALAXY REDSHIFT SURVEY FROM SUBHALO ABUNDANCE AND ENVIRONMENT MATCHING

BRIAN F. GERKE^{1,*}, RISA H. WECHSLER^{1,2}, PETER S. BEHROOZI^{1,2}, MICHAEL C. COOPER³, RENBIN YAN⁴, ALISON L. COIL⁵

Draft version October 16, 2018

ABSTRACT

We develop empirical methods for modeling the galaxy population and populating cosmological N -body simulations with mock galaxies according to the observed properties of galaxies in survey data. We use these techniques to produce a new set of mock catalogs for the DEEP2 Galaxy Redshift Survey based on the output of the high-resolution Bolshoi simulation, as well as two other simulations with different cosmological parameters, all of which we release for public use. The mock-catalog creation technique uses subhalo abundance matching to assign galaxy luminosities to simulated dark-matter halos. It then adds color information to the resulting mock galaxies in a manner that depends on the local galaxy density, in order to reproduce the measured color-environment relation in the data. In the course of constructing the catalogs, we test various models for including scatter in the relation between halo mass and galaxy luminosity, within the abundance-matching framework. We find that there is no constant-scatter model that can simultaneously reproduce both the luminosity function and the autocorrelation function of DEEP2. This result has implications for galaxy-formation theory, and it restricts the range of contexts in which the mocks can be usefully applied. Nevertheless, careful comparisons show that our new mocks accurately reproduce a wide range of the other properties of the DEEP2 catalog, suggesting that they can be used to gain a detailed understanding of various selection effects in DEEP2.

Subject headings: galaxies: evolution — galaxies: high-redshift — large-scale structure of the universe — galaxies:halos — dark matter

1. INTRODUCTION

The accurate interpretation of galaxy survey data requires a careful consideration of a wide range of biases and incompleteness that can arise from the selection of the surveyed galaxies. Galaxy selection most commonly occurs as a function of galaxy flux, color, and (particularly for spectroscopic surveys) local density on the sky. Since these three properties are well known to be strongly correlated with one another (*e.g.* Hogg et al. 2004; Cooper et al. 2006), a selection algorithm that chooses galaxies based on one of them will also produce selection biases in the distributions of the others. Estimating the scale of secondary selection effects like these requires a detailed understanding of the interplay between different galaxy properties; this becomes more important and more complex when considering surveys that cover a wide range in redshift, since the galaxy population may evolve substantially

over the lookback time of the survey. The use of mock (*i.e.*, simulated) galaxy catalogs to understand and account for selection effects has therefore been an important part of the analysis in nearly all modern galaxy surveys, particularly those probing redshifts of order unity, such as DEEP2 (Davis et al. 2003; Newman et al. 2012), VVDS (Le Fèvre et al. 2005), and zCOSMOS (Lilly et al. 2009).

In this study, we develop a set of empirically based techniques for constructing mock galaxy catalogs for high-redshift surveys. We also produce a new set of catalogs for the DEEP2 survey and make them available to the public, although our techniques should be generally applicable to any spectroscopic galaxy survey. One of our primary goals in constructing the mock catalogs presented here is to produce a simulated catalog appropriate for testing and optimizing algorithms to detect groups and clusters of galaxies in redshift space in DEEP2. We also wish to use these mocks to calibrate the halo-mass selection function that corresponds to the observational selection of galaxy groups (*i.e.*, systems with two or more observed members in DEEP2).

At present, the detailed astrophysics of galaxy formation is not sufficiently well understood to directly simulate the galaxy population from first principles. However, there is strong support, through many different lines of evidence, for a basic picture of galaxy formation which holds that (1) all galaxies are embedded in larger dark matter halos that comprise most of their mass, (2) above some minimum mass threshold, all dark matter halos (whether primary halos or subhalos within a primary) host a single galaxy at their centers, and (3) there is a tight relation between the optical luminosity of a galaxy

bgerke@slac.stanford.edu

¹Kavli Institute for Particle Astrophysics and Cosmology, SLAC National Accelerator Laboratory, M/S 29, 2575 Sand Hill Rd., Menlo Park, CA 94025

²Department of Physics, Stanford University, Stanford, CA, 94305

³Center for Galaxy Evolution, Department of Physics and Astronomy, University of California–Irvine, Irvine, CA 92697

⁴Center for Cosmology and Particle Physics, Department of Physics, New York University, 4 Washington Place, New York, NY 10003

⁵Center for Astrophysics and Space Sciences, University of California, San Diego, 9500 Gilman Dr., MC 0424, La Jolla, CA 92093

* Current address: Energy Efficiency Standards Group, Lawrence Berkeley National Laboratory, 1 Cyclotron Rd., M/S 90R4000, Berkeley CA 94720

and the mass of its dark matter host. This paradigm suggests an obvious approach to constructing mock galaxy catalogs by assigning a galaxy properties to each halo or subhalo in a dark-matter-only N-body simulation, using some prescription for mapping between galaxy properties and (sub)halo properties. Techniques for converting periodic N-body simulation volumes into the cone-shaped geometries typical of surveys, and for including the effects of cosmic structure evolution at high redshift, are now well developed (*e.g.*, Yan, White, & Coil 2004; Blaizot et al. 2005; Kitzbichler & White 2007). What remains is to specify a halo-galaxy connection that reproduces the observed galaxy population with high accuracy.

One would ideally like to have a physically well-motivated method for assigning galaxies to dark-matter halos, so numerous authors have constructed mocks using semi-analytic models of galaxy formation applied to the underlying N-body simulations (*e.g.*, Eke et al. 2004; Kitzbichler & White 2007; Henriques et al. 2012). At present, however, most such models fail to accurately reproduce the color distribution of galaxies at redshifts near unity. An additional difficulty arises because, until quite recently, N-body simulations of cosmologically interesting volumes have not had sufficient particle numbers to resolve the relatively low-mass halos and subhalos that host the faintest galaxies in modern surveys. Yan, White, & Coil (2004) (hereafter YWC) addressed these problems by taking an empirically based halo-model approach, using a conditional luminosity function to construct mock catalogs for the DEEP2 redshift survey, populating massive halos with one central galaxy and a number of satellites depending on the halo mass, in such a way as to match the measured DEEP2 luminosity and autocorrelation functions. Since the satellites had to be randomly assigned to dark matter particles in these halos, rather than to well-defined subhalos, this approach likely mis-estimated the spatial profiles and velocity distributions of galaxy groups and clusters. Given the simulations available at the time, however, even this approach could only account for the relatively bright galaxies probed by DEEP2 at $z \gtrsim 0.7$; the fainter galaxy population sampled at low z was not included.

The YWC mocks also did not include information on galaxy properties besides luminosity, although Gerke et al. (2007) were able to add color information to these mocks according to the measured relation between color and local galaxy density. Their approach to color assignment was inspired by the ADDGALS mock-catalog creation algorithm that was used to produce mock catalogs for the Sloan Digital Sky Survey (York et al. 2000) in *e.g.*, Koester et al. (2007a), and which will be described in detail by Wechsler et al. (in preparation). Even with the addition of colors, these mocks were not sufficient to model the faint, low-redshift population probed by DEEP2 in one of its three observational fields. In addition, the YWC mocks were based on N-body simulations whose underlying cosmological parameters are at variance with the best fit to current data. For these reasons, we are motivated to improve upon the YWC efforts and construct new mock catalogs for the DEEP2 survey.

Since the construction of the YWC mocks, improvements in both software and hardware have allowed for a substantial increase in the mass resolution of N-body simulations of a given volume. Most recently, the

Bolshoi simulation (Klypin, Trujillo-Gomez, & Primack 2011) simulated the growth of cosmic structure in a cubical volume 250 comoving h^{-1} Mpc on a side, resolving halos and subhalos down to masses smaller than those of the Magellanic Clouds (Busha et al. 2011) and using a set of cosmological parameters that is in good agreement with current constraints from a wide variety of data. The combination of a large volume and excellent mass resolution permit the construction of DEEP2 mock catalogs over the full redshift and luminosity range probed by the survey, except for a handful of very faint low- z dwarfs. Moreover, because Bolshoi resolves subhalos down to the required mass range for DEEP2, we will be able to assign galaxies to halos and subhalos individually, rather than taking a halo-model based approach, which should better reflect the phase-space distributions of galaxies in groups and clusters.

Lacking a sufficiently accurate astrophysical model of galaxy formation, we carry on with a purely empirical approach to mock-catalog construction. A popular technique for assigning galaxy luminosities, known as subhalo abundance matching, has been demonstrated as a feasible means of reproducing both the galaxy luminosity function and the autocorrelation function at a variety of redshifts, under certain cosmological assumptions (*e.g.* Kravtsov et al. 2004; Tasitsiomi et al. 2004; Vale & Ostriker 2004; Conroy, Wechsler, & Kravtsov 2006; Reddick et al. 2013); we adopt this approach here and explore its applicability in more detail. To add color information to the resulting mock catalogs, we expand on the environment-dependent approach of Gerke et al. (2007), making substantial improvements to accurately model galaxies near the DEEP2 flux limit, as well as various luminosity and color-dependent sources of incompleteness in the survey. We also repeat the mock-making procedure for two other high-resolution N-body simulations with different cosmological parameters from Bolshoi, to facilitate tests for cosmological dependence in the DEEP2 selection function.

We proceed as follows. The next section introduces the DEEP2 survey and the N-body simulations. Section 3 details our methods for assigning galaxy properties to halos and subhalos, while Section 4 describes the techniques we use to replicate various DEEP2 selection effects in the resulting catalogs. Section 5 is likely the most useful portion of the paper for users of these mock catalogs, since it makes detailed comparisons between the mock catalogs and the DEEP2 dataset. In the Appendix, we describe the contents of the public DEEP2 mock catalogs and give a brief example of their use for computing the DEEP2 halo-mass selection function. Throughout this paper, unless otherwise specified, distances are quoted in comoving h^{-1} Mpc and absolute magnitude values are given as $M - 5 \log h$.

2. DATA AND SIMULATIONS

2.1. The DEEP2 Galaxy Redshift Survey

The DEEP2 (Deep Extragalactic Evolutionary Probe 2) Galaxy Redshift Survey is a large spectroscopic survey of galaxies at $z \sim 1$ comprising spectra of some 50,000 objects and $\sim 35,000$ confirmed galaxy redshifts in four observational fields covering a total of $\sim 3 \text{ deg}^2$ on the sky. Complete details of the survey, including tar-

get selection, spectroscopy, data reduction, and redshift assignment procedures appear in Newman et al. (2012); substantial discussion of these issues is also available in Davis, Gerke, & Newman (2004); Davis et al. (2007), and Willmer et al. (2006) (hereafter W06). Here, we summarize the properties of the survey that we will need to replicate in our mock catalogs.

Spectroscopic targets for DEEP2 were selected from deep imaging with the CFH12k camera on the Canada-France-Hawaii telescope (Coil et al. 2004) in the B , R and I bands. Three of the four fields each comprise three CFH12k pointings, oriented along lines of constant declination, making a 1 deg^2 contiguous field with a $2 \text{ deg} \times 0.5 \text{ deg}$ aspect ratio. The fourth field is the $2 \text{ deg} \times 0.25 \text{ deg}$ Extended Groth Strip (EGS), which is oriented perpendicular to the ecliptic and has been the site of a wide variety of observations across the full range of the electromagnetic spectrum.

The spectroscopic selection has an R -band apparent magnitude limit of 24.1, and a selection in observed color-color space was also applied to exclude galaxies at redshifts below $z \sim 0.75$, except in the EGS, where galaxies were observed throughout color space, but with a preference for galaxies expected to lie at $z > 0.75$. Spectra were obtained with the DEIMOS spectrograph (Faber et al. 2003) on the Keck II telescope, which uses custom-milled slitmasks to allow multiplexed slit spectroscopy of $\gtrsim 100$ objects simultaneously. The DEEP2 spectroscopic targeting algorithm tiles the DEEP2 fields with DEIMOS slitmasks in an overlapping pattern such that most of the suitable galaxies have at least two chances of being selected for spectroscopy (four chances in the EGS). Because the total slit length available is limited, it is not possible to target all suitable galaxies for spectroscopy; the targeting efficiency of DEEP2 is $\sim 60\%$.

Data reduction and initial redshift estimation was performed using a software pipeline (Newman et al. 2012) that was specially designed for use with DEEP2 DEIMOS data. Each spectrum was then examined by eye and the initial redshift estimate was either confirmed or corrected, or the spectrum was rejected as a failure. Roughly 70% of DEEP2 spectra yield successful redshifts. We estimate, however, that $\sim 15\%$ of DEEP2 targets lie beyond the DEEP2 target redshift range (C. Steidel 2003, private communication), at $z > 1.4$, where all useful spectral features for redshift identification have shifted out of the optical waveband. Thus, the redshift-success rate for DEEP2 galaxies in the appropriate redshift range is $\sim 85\%$; when combined with the targeting rate, this gives an overall spectroscopic sampling rate for DEEP2 of $\sim 50\%$.

2.2. *N-Body Simulations*

We use dark matter halos from three N-body simulations. Our principal results use the Bolshoi simulation (Klypin, Trujillo-Gomez, & Primack 2011), which modeled a $250 h^{-1} \text{ Mpc}$ comoving box with $\Omega_m = 0.27$, $\Omega_\Lambda = 0.73$, $\sigma_8 = 0.82$, $n = 0.95$, and $h = 0.7$. The simulation volume contained 2048^3 particles, each with mass $1.15 \times 10^8 h^{-1} M_\odot$, and was run using the ART code (Kravtsov, Klypin, & Khokhlov 1997). Halos and subhalos were identified using the BDM algorithm (Klypin & Holtzman 1997); see Klypin, Trujillo-Gomez, & Primack (2011) for details.

This simulation’s spatial resolution is a physical scale of $1 h^{-1} \text{ kpc}$. This improves the tracking of halos as they merge with and are disrupted by larger objects, allowing them to be followed even as they pass near the core of the halo. The resulting halo catalog is nearly complete for objects down to a circular velocity of $v_{\text{max}} = 55 \text{ km s}^{-1}$. Merger trees were created using the consistent merger tree code of Behroozi et al. (2013).

The additional simulations used are described in Table 1. These simulations were also run with the ART code and analyzed in the same way as Bolshoi; we primarily use them to test the impact of varying cosmological parameters on the properties of our mock catalogs. All results shown use the Bolshoi simulation, with the exception of Figure 12, which compares the halo occupation distribution between the simulations.

3. MOCK-CATALOG CREATION ALGORITHM

A brief summary of our algorithm for constructing DEEP2 mock catalogs from the N-body simulations is as follows. We first construct redshift-space lightcones with the geometry of the DEEP2 by defining an observer position and line-of-sight direction in the $z = 0$ simulation output and then stacking different simulation outputs along the line of sight, making use of the boxes’ periodic boundary conditions. We then assign monochromatic (B -band) galaxy luminosities to the dark matter halos and subhalos, according to the measured DEEP2 luminosity function, using the subhalo abundance matching technique (*e.g.* Conroy, Wechsler, & Kravtsov 2006; Behroozi, Conroy, & Wechsler 2010), and we account for the measured redshift evolution in this luminosity function. We assign each mock galaxy a $U - B$ color drawn from the DEEP2 survey according to its local density, by matching the color distribution in quintiles of local density between DEEP2 and the mock catalog, and we apply an inverse k -correction to these galaxies to obtain an observed R -band apparent magnitude for each one. Finally, we apply the various DEEP2 selection cuts, including density-dependent incompleteness arising from the scheduling of galaxies for DEIMOS spectroscopic observation and color, luminosity, and redshift-dependent incompleteness arising from the failure to obtain reliable redshifts for some targets. We explain each of these steps in detail in the following sections.

3.1. *Constructing the lightcone*

To construct a realistic mock catalog, it is necessary to convert the real-space positions of halos and subhalos in an N-body simulation into redshift-space positions in a lightcone that conforms to the survey geometry. To the extent possible, we would also like the positions at each redshift to correspond to the appropriate epoch of the simulation—so that, for example, mock galaxies at $z = 1$ are drawn from a snapshot of the simulation at a scale factor $a = 0.5$. Since we would like our lightcones to represent the DEEP2 survey volume as realistically as possible, we wish to avoid duplicating any region of the simulation volume in any one lightcone. Numerous authors have implemented lightcone-making for mock catalogs (*e.g.*, YWC, Blaizot et al. 2005; Kitzbichler & White 2007). Here, in the two smaller simulation boxes (120 and 160 Mpc), we

closely follow the approach of YWC. In the Bolshoi simulation, owing to the larger volume available, we take a somewhat more flexible approach. We outline these lightcone-construction algorithms briefly below.

The basic idea is to choose an observer position within the simulation box, an observational field geometry, and a direction of observation. We can then trace a cone through the box, making use of the periodic boundary conditions of the simulation to “wrap” the lightcone and construct a line of sight that is significantly longer than the nominal dimensions of the box. Once the cone is constructed, it is straightforward to convert the positions of halos and subhalos in the simulation box into RA, Dec and line-of-sight distance coordinates in the lightcone. We then convert the line-of-sight distance into a redshift for each object using the distance–redshift relation for the background cosmology of the mock and adding a peculiar-velocity contribution derived from the velocity component of each object along the chosen line of sight. In each simulation, we include halos and subhalos down to masses of a few times $10^9 M_\odot$, which includes the mass range of the faint ($M_B > -15$) dwarf galaxies that DEEP2 probes at low redshift in the EGS. In some simulations, including Bolshoi, the halo population is incomplete at these masses, but low-mass dwarfs only appear at very low redshift in the EGS field of DEEP2, and this part of DEEP2 probes an exceedingly small volume. Such incompleteness will thus only have a very minor impact on projection effects, and will not impact any cosmological comparisons.

It is important to take some care in the choice of line-of-sight direction, angling it to ensure that the lightcone does not overlap itself on subsequent passes through the simulation box and repeatedly sample the same volume (see, *e.g.*, the bottom panel in Figure 2 of Blaizot et al. 2005). This also imposes a practical limit on the redshift range that a given lightcone can probe, which depends on the geometry of the observational field: a wide lightcone will quickly reach a comoving transverse size similar to the box size for example, making overlaps inevitable. Since DEEP2 is nearly a pencil-beam survey, however (the fields are ~ 2 degrees across in the longest dimension), this is not a limitation for our purposes in practice.

YWC used a simulation whose output timestep spacing corresponded to the light-travel time over roughly half of the simulation box dimensions. Their approach to constructing lightcones was to start with an observer position on one face of the simulation cube and transition between timesteps each time the line of sight had traversed half of the box. It is then possible to make a second lightcone by translating the observer position halfway across the box in the direction perpendicular to the face that was chosen initially. This procedure can be repeated for each of the six box faces, allowing a maximum of twelve lightcones to be constructed. If more lightcones or a finer time-spacing are desired, it is possible to generalize this approach to start with a randomly selected observer location and sightline, subject to the requirement that the lightcone not overlap itself (*e.g.* Kitzbichler & White 2007).

How many lightcones should we produce for each simulation? Since we would like to use our mock catalogs to estimate the sample variance in DEEP2, we would like our lightcones to probe independent (*i.e.*, nonoverlap-

ping) volumes as much as is possible. In the ideal case, all of our mock lightcones would contain completely independent volumes, and so we should stop constructing lightcones once their total volume equals the volume of the simulation box⁷. For many purposes, however, it is sufficient if the mocks are independent only at fixed redshift, or, more precisely, in redshift bins of the width that we are typically interested in considering in our analyses. That is, if we want to estimate the sample variance in bins of width $\Delta z = 0.1$, then it is acceptable if mock *A* contains the same volume at $z = 1$ that mock *B* contains at $z = 0.5$. For this reason, we will tend to “overfill” our simulation boxes with mock catalogs by a factor of a few, to allow for better statistical power in estimating the sample variance in redshift bins.

A single 1 deg^2 DEEP2 observational field contains a total volume of $\sim 2 \times 10^6 h^{-3} \text{ Mpc}^3$ over the primary DEEP2 redshift range of $0.75 < z < 1.4$, and a redshift bin of width $\Delta z = 0.1$ has a volume $\sim 3 \times 10^5 h^{-3} \text{ Mpc}^3$. Thus, we can fit one complete DEEP2 field into the L120 simulation, and two into the L160 box, and on the order of ten independent $\Delta z \sim 0.1$ redshift bins into each. We therefore use exactly the algorithm that was used in YWC to construct lightcones for these two boxes, producing twelve lightcones for each box. Given the total volume of the boxes, we expect that redshift bins of width 0.125 will contain independent volumes across all twelve cones in the L160 box, and bins of width 0.05 will be independent across the L120 lightcones. These numbers are summarized in Table 1. In each case, wider bins will allow proportionally fewer independent cones. Both of these simulations have sufficient time resolution in their outputs that we can follow the YWC technique of transitioning between timesteps whenever the sightline has traversed half the box—except in the case of the L120 box at $z > 1$. In that regime, there are only a few simulation outputs covering the entire range from $1.0 < z < 1.4$. For this reason, we advise against using the L120 box for applications that require an accurate representation of the redshift evolution of cosmic structure.

The larger volume of the $250 h^{-1} \text{ Mpc}$ Bolshoi simulation allows us to construct significantly more independent DEEP2 samples, with the volume of eight fully independent DEEP2 fields (over the primary $0.75 < z < 1.4$ redshift range) available in Bolshoi, and scores of independent $\Delta z \sim 0.1$ redshift bins available. We therefore use the more flexible approach to lightcone-building described above, with randomly selected observer positions and lines of sight, to construct forty DEEP2 lightcones from the Bolshoi simulation. These forty lightcones should be almost completely independent in redshift bins as wide as 0.15. The time resolution of Bolshoi is sufficiently good over the entire redshift range sampled to allow multiple timesteps to be used in each crossing of the box, so the growth of large-scale structure should be captured with sufficient accuracy for any practical purposes.

⁷ Neither of our algorithms absolutely guarantees that two different lightcones will not overlap, of course, but since DEEP2 is nearly a pencil-beam survey, any overlapping volume between mocks should be small.

Table 1

Parameters of the three N-body simulations used to produce mock catalogs in this work.

| Simulation | Box Dimension (h^{-1} Mpc) | Ω_M | σ_8 | h | # of lightcones | # independent DEEP2 fields | Max. independent z bin width ^a |
|------------|----------------------------------|------------|------------|------|--------------------|-------------------------------|--|
| L120 | 120 | 0.3 | 0.7 | 0.73 | 12 | 1 | 0.05 |
| L160 | 160 | 0.24 | 0.9 | 0.7 | 12 | 2 | 0.15 |
| Bolshoi | 250 | 0.27 | 0.82 | 0.7 | 40 | 8 | 0.15 |

^a So that, for example the same redshift bin in the L160 lightcones samples a different region of space in all twelve cones.

3.2. Luminosity assignment by subhalo abundance matching

As discussed in the introduction, one of our primary goals is to produce a catalog that can be used for testing and calibrating group-finding algorithms. Therefore, we want to ensure that our mock catalogs accurately reproduce both the *number* of observed galaxies in massive halos and their *distribution* in phase space, since redshift-space cluster-finding algorithms will be strongly sensitive to both of these.

3.2.1. Subhalo abundance matching: rationale and basic approach

In the language of the halo model, our first requirement translates to accurately reproducing the halo occupation probability, $P(N|M)$, which is the probability that N galaxies brighter than some luminosity threshold dwell in a halo of mass M . This distribution is typically represented by its first moment, $\bar{N}(M)$, typically called the halo occupation distribution (HOD), plus an assumed form for the scatter in N (see, *e.g.*, Zheng et al. 2005). For a given background cosmology, a particular choice of HOD uniquely specifies the two-point autocorrelation function of galaxies (Peacock & Smith 2000). If we assume our simulation has the correct background cosmology, we can choose a prescription for populating it with mock galaxies and test the accuracy of the HOD by comparing its correlation function to the one measured in the DEEP2 data. YWC took this basic approach: they assigned galaxies to massive dark matter halos as a function of mass according to a conditional luminosity function (CLF; see *e.g.* Yang, Mo, & van den Bosch 2003), $\phi(L|M)$. It was possible to tune the CLF to reproduce the observed DEEP2 galaxy clustering and, once this was achieved, to have some confidence that the resulting HOD in the mocks was an accurate representation of the DEEP2 HOD⁸.

However, the N-body simulations YWC used did not have sufficiently high resolution to include the low-mass subhalos that would be expected to host the faintest DEEP2 galaxies in groups. Thus, instead of placing all galaxies in halos or subhalos, those authors assigned a single galaxy to the center of each halo and satellite galaxies to the positions and velocities of dark-matter particles selected at random from the halo. Since the

distribution of galaxies within a cluster is unlikely to perfectly trace the dark matter distribution, this approach will produce inaccuracies in the phase-space distribution of galaxies on small spatial scales. Put another way, the YWC mocks do not include the effects of luminosity-dependent galaxy bias (except to the extent that the brightest galaxy in each halo was placed at the center). This could have important implications for cluster finding if bright galaxies in clusters have a significantly different spatial or velocity distribution than faint ones. (Indeed, Coil et al. (006a) showed that radial distribution of galaxies in halos in the YWC mocks was not consistent with the DEEP2 data.)

For this reason, we have been careful in this work to choose high-resolution N-body simulations in which the lowest-mass halos and subhalos have a number density that matches or exceeds that of the faintest galaxies observed in DEEP2. This will permit us to assign all galaxies directly to the centers of halos and subhalos and thus, presumably, to more accurately reproduce the phase-space distribution of DEEP2 galaxies. This also allows us to bypass the step of selecting a CLF or HOD and tuning it to match the DEEP2 correlation function. Instead, we can construct a direct relation between a galaxy's luminosity and the properties of its host halo or subhalo, choosing this relation in such a way as to reproduce the DEEP2 clustering results.

The simplest way to construct such a relation is to match the luminosity function of galaxies directly to the mass function of subhalos at fixed number density, which is the core of the abundance matching technique. More precisely, we integrate the luminosity function to compute the number density of galaxies brighter than some luminosity, $n(>L) = \int_L^\infty \phi(L)dL$ and compare it to the number density of halos and subhalos more massive than some mass, $n(>M)$ (under a particular choice of halo-mass definition)⁹. Setting $n(>L) = n(>M)$ then yields an implicit relation between luminosity and mass, $L(M)$ that must obtain if a galaxy's luminosity depends only on the mass of its host halo. In reality, although there is strong evidence for a tight relation between galaxy luminosity and halo mass, there are numerous other factors that can affect galaxy luminosity at fixed mass, so some scatter in this relation is to be expected. In any event, a particular implicit mean $L(M)$ relation and scatter about that relation will correspond to a particular HOD, and hence a particular galaxy autocorrelation function, since the subhalos of massive halos will be populated by more

⁸ However, the comparison between the two-point functions of the mocks and the data was performed using early DEEP2 measurements with large uncertainties. More recent measurements of the DEEP2 clustering are not consistent with the YWC mocks, sharpening the need for a new set of catalogs. In addition, the background cosmology in the YWC mocks is no longer consistent with present data.

⁹ It is worth noting here that we always compute $n(M)$ over the entire simulation box, rather than for the lightcones individually, to minimize the effects of sample variance on our abundance-matching procedure.

or fewer bright galaxies depending on the details of the chosen relation. If we assume that the basic picture of a tight $L(M)$ relation with some scatter is correct, then we can extract this relation from the data by populating subhalos in a simulation according to such a relation and varying the details (*e.g.*, the size of the scatter or the subhalo mass definition) until we obtain an autocorrelation function in the simulation that matches the measured one.

Conroy, Wechsler, & Kravtsov (2006) showed that the basic features of the measured autocorrelation function could be reproduced using this technique, both at low redshifts, from SDSS, and at high redshifts, from DEEP2, given two minor alterations to the basic algorithm described above. First, they used the maximum circular velocity values, v_{\max} , of the halos, rather than their masses, to compute their number density function (v_{\max} is a more robust tracer of halo mass than the total mass of the particles in the halo, because it traces the central part of the halo which is less sensitive to tidal stripping (Kravtsov et al. 2004; Muldrew, Pearce, & Power 2011; Knebe et al. 2011)). In addition, when a halo was in fact a subhalo of a more massive object, they assigned it the v_{\max} value it had at the time it was accreted into the larger halo, v_{\max}^{acc} , for the purposes of computing halo number density. That is, they used abundance matching to derive an implicit $L(v_{\max}^{\text{acc}})$ relation. The choice of the accretion-time v_{\max} amounts roughly to assuming that satellite galaxies falling into larger groups or clusters of galaxies are stripped of their outer dark matter halos but not stripped of stars, so that after they are accreted their luminosities are higher than the mean $L(v_{\max})$ relation for distinct halos. Conroy, Wechsler, & Kravtsov (2006) found that ignoring this effect led to a too-low correlation function on small scales.

3.2.2. Testing the impact of scatter

Introducing scatter into the $L(v_{\max}^{\text{acc}})$ relation generally has the effect of reducing the spatial correlation of the mock galaxies. This is because the mass function is steeply falling, so that there is always a much larger population of lower-mass halos than higher-mass ones for a given reference mass, so scatter in luminosity at fixed mass will include a large number of low-mass halos in the population brighter than a given luminosity, compared to the scatter-free case. Since halo bias (the ratio of the halo correlation function to the dark-matter one) is an increasing function of mass, including low-mass halos will suppress the clustering. Reddick et al (in preparation) found that the subhalo abundance matching approach yields the best match to the SDSS autocorrelation function and conditional luminosity function if the $L(v_{\text{peak}})$ relation used has a scatter in luminosity at fixed halo circular velocity (using the maximum value of this circular velocity over each halo’s history, v_{peak}), with a scatter of ~ 0.18 dex yielding the best results.

To investigate the appropriate scatter to use for reproducing the DEEP2 autocorrelation function, we choose the output of the Bolshoi simulation at $a = 0.528$ (corresponding to $z = 0.9$, near the peak of the DEEP2 redshift distribution) and use abundance matching to populate its halos and subhalos with galaxies drawn from the $z = 0.9$ DEEP2 luminosity function measured by W06.

We repeat this exercise with various different amounts of log-normal scatter in the implicit $L(v_{\max}^{\text{acc}})$ relation, from 0 to 0.6 dex; in each case the scatter is constant as a function of v_{\max}^{acc} . We then compute the projected correlation function, $w_p(r_p)$, as viewed along one axis of the box, and we compare with the measured values in DEEP2 (Coil et al. 006b), for galaxies brighter than a two different thresholds in luminosity.

The scatter model is implemented by an iterative non-parametric forward convolution method, as in Behroozi, Conroy, & Wechsler (2010). A fiducial guess for the deconvolved median $L(v_{\max}^{\text{acc}})$ relation is obtained by abundance matching the luminosity function to halos with zero scatter. This relation is then convolved with the desired scatter model to generate fiducial halo luminosities. Abundance matching is repeated; instead of matching the brightest galaxy to the halo with the greatest v_{\max}^{acc} , however, the brightest galaxy is matched to the halo with the highest fiducial luminosity. This in turn generates a new fiducial median $L(v_{\max}^{\text{acc}})$ relation, which can again be convolved with the scatter model to generate new fiducial luminosities. After several iterations, this deconvolution approach converges to a stable relation for the underlying median $L(v_{\max}^{\text{acc}})$ relation if it exists, along with the distribution of halo v_{\max} with luminosity (i.e., $P(v_{\max}^{\text{acc}}|L)$).

Because no assumptions about the scatter model are made in this process, we may explore a variety of models. However, not all scatter models are “allowed” in the sense that the steep fall-off of the luminosity function imposes a stringent limit on the scatter for luminous galaxies. Even if the underlying relation for $L(v_{\max}^{\text{acc}})$ imposed a sharp maximum limit on the luminosity, the addition of log-normal scatter would broaden the fall-off in the luminosity function; for DEEP2, this broadening becomes inconsistent with the observed fall-off for constant scatter models above 0.3 dex. In these circumstances, our implementation recovers a solution for $L(v_{\max}^{\text{acc}})$ which, when convolved with the scatter model, cannot match the luminosity function at the luminous end, and so only approximately matches the luminosity function at lower luminosities as well.

Figure 1 shows the comparison for absolute magnitudes $M_B \leq -19$ and $M_B \leq -20$. Open data points denote the projected correlation functions we obtain from the abundance-matched Bolshoi simulation with different assumed values for the scatter. Error bars are computed using jackknife sampling in the box; hence they include the impact of cosmic variance on scales smaller than the box (in the Figure they have been suppressed for all but the zero-scatter model, to reduce clutter). Black solid data points show the $w_p(r_p)$ measurements of Coil et al. (006b). The solid line shows the best-fitting power representation of the clustering obtained over all scales in that work, and the dashed and dotted lines show the best fits on scales larger and smaller than 1 Mpc, respectively. The lower panels show the fractional difference between the best fit to the data (solid line) and the results of the abundance-matching exercise with different amounts of scatter.

Substantial scatter appears to be needed to reproduce the DEEP2 clustering results to good accuracy: for scatter values below 0.4 dex, the abundance-matched Bolshoi catalog is significantly more clustered than DEEP2 for all

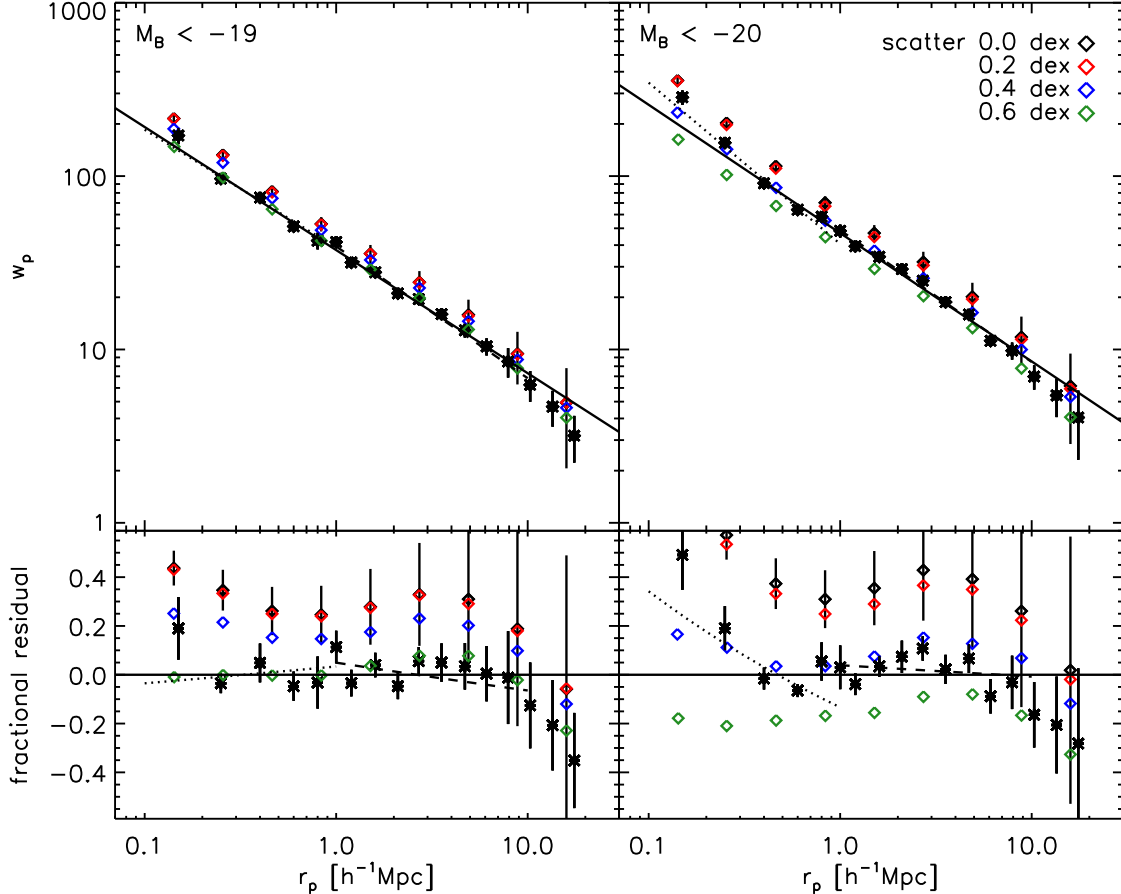


Figure 1. Comparison of the projected autocorrelation functions, $w_p(r_p)$ in DEEP2 and in our abundance matching populations of the Bolshoi simulation with different amounts of scatter, for two different absolute magnitude thresholds. Black points show the DEEP2 clustering results (Coil et al. 006b), and the solid, dashed, and dotted lines show the best-fitting power laws to those data for all scales and scales greater than and less than 1 Mpc, respectively. The colored points denote the clustering measured in the Bolshoi simulation at $z \sim 0.9$ after abundance-matching to the DEEP2 B -band luminosity function, assuming various amounts of scatter in the $L(v_{\text{max}}^{\text{acc}})$ relation, as shown in the legend. Error bars on the colored points have been suppressed for all but one of the scatter values to reduce clutter. There is little significant effect on clustering for scatter below 0.2 dex, and all such models are more strongly clustered than the DEEP2 data. Higher values of the scatter produce more significant impacts on the clustering, but no value of the scatter is consistent with the DEEP2 data at all luminosity thresholds.

threshold luminosities. This suggests that the results of Conroy, Wechsler, & Kravtsov (2006), who matched the DEEP2 clustering with a zero-scatter abundance matching model, were an accident of their having used a simulation whose background cosmology had a high value of σ_8 . For higher values of the scatter, we find that it is possible to reproduce the DEEP2 two-point function for a given threshold luminosity, with a scatter of 0.4 dex being sufficient for $M_B < -20$ and 0.6 dex working well for $M_B < -19$, but there is no fixed-scatter model that reproduces the Coil et al. (006b) results for all threshold luminosities. We note in passing that this outcome is in qualitative agreement with the study by Wetzel & White (2010), who found that a scatter of ~ 0.6 dex was required to approximately match the DEEP2 clustering results with an abundance matching approach. Nevertheless, the lack of a single scatter value that consistently matches the DEEP2 clustering at all luminosity thresholds suggests that this fixed-scatter abundance matching approach may be too simplistic to account for the true galaxy population at high redshift, at least for samples

selected in the B-band.

In fact, the inconsistency is worse than it appears in Figure 1. As mentioned above, our technique for adding scatter to the abundance matching approach does not necessarily guarantee that the output mock galaxy catalog will match the desired luminosity function. Figure 2 shows the luminosity function we obtain from the model Bolshoi catalog for the same scatter models discussed above (colored points), compared to the W06 luminosity function that we used as input to the abundance matching algorithm. The models with 0.2 dex scatter and below match the input luminosity function well, but models with higher scatter deviate significantly from the W06 function at bright luminosities. The reason for the discrepancy is straightforward to understand. The output luminosity function from our abundance matching algorithm is effectively a convolution between the log-normal scatter and an implicit no-scatter luminosity function, which must necessarily be steeper at the bright end than the input DEEP2 luminosity function, which is itself already quite steep. At some value for the scatter, the

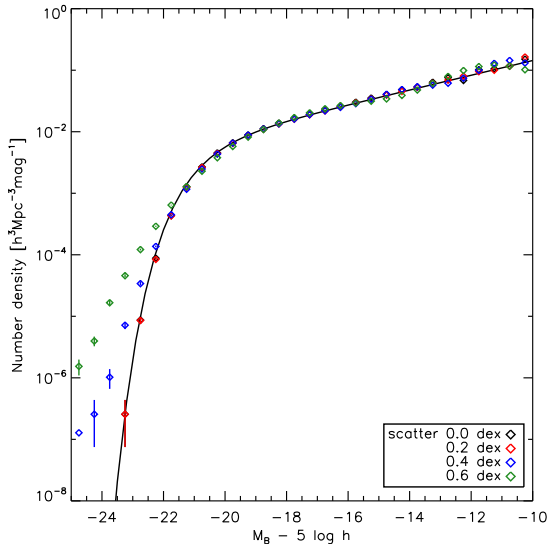


Figure 2. A comparison of the input DEEP2 luminosity function (solid line) to the actual luminosity functions achieved in the various scatter scenarios for abundance matching shown in Figure 1. The error bars shown for the mock scenarios reflect Poisson uncertainty. For scatter of $\lesssim 0.2$ dex in luminosity at fixed v_{\max}^{acc} , the input luminosity function is reproduced accurately, but for larger values of the scatter, the output catalog contains too many bright $L >^*$ galaxies, indicating that such large values of the scatter in a fixed-scatter abundance matching approach are inconsistent with the DEEP2 luminosity function, given the Bolshoi cosmology.

required no-scatter luminosity function will have an infinite slope at the bright end, and for larger values of the scatter it will be impossible to reproduce the DEEP2 luminosity function.

Figure 2 therefore suggests that the maximum fixed log-normal scatter for abundance matching that is consistent with the W06 DEEP2 luminosity function is ~ 0.2 dex in luminosity at fixed v_{\max}^{acc} . Given that no such model is consistent with the DEEP2 correlation function, we conclude that the simple fixed-scatter abundance matching technique for connecting galaxies with dark-matter halos is inconsistent with DEEP2 data in detail. It is worth noting that the DEEP2 luminosity function is measured in the rest-frame B band, which is sensitive to transient effects like starbursts and AGN, whereas the SDSS luminosity function that has been reproduced by fixed-scatter abundance matching is measured in the r band, which should be less sensitive to such effects. In any case, the fact that the DEEP2 luminosity-function discrepancy is limited to bright magnitudes, coupled with the varying amounts of scatter required to match the clustering for different luminosity thresholds, suggest that a variable-scatter abundance matching model whose scatter decreases as a function of v_{\max}^{acc} might yield consistency with all of the DEEP2 measurements. One such model has been recently described by Trujillo-Gomez et al. (2011), which forces agreement with the input luminosity function at the expense of non-constant scatter. This model is not a unique solution, and the possible form and parameters of models with non-constant scatter are unclear, so a detailed exploration of these issues is outside the scope of this work.

In order to proceed, then, we must choose between an accurate luminosity function and an accurate two-point

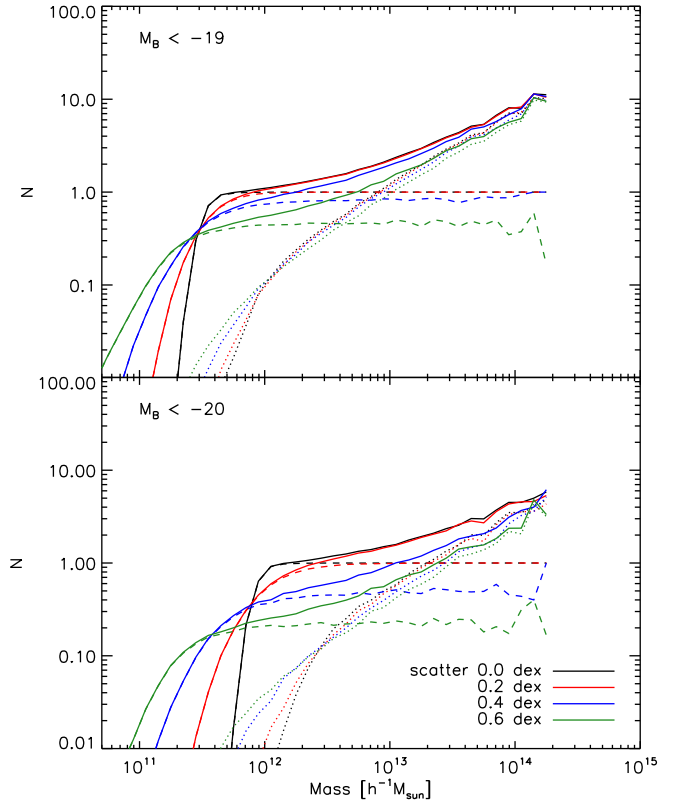


Figure 3. The halo occupation distributions (HODs) that result from applying each of the scatter values for abundance matching in Figure 1 to the Bolshoi simulation. Solid lines show the mean number of galaxies per halo $\bar{N}(M)$, and dashed and dotted lines show the mean numbers of central and satellite galaxies, respectively. For scatter values larger than 0.2 dex in luminosity at fixed v_{\max}^{acc} , the mean number of central galaxies remains below unity at all masses, which is radically inconsistent with current understanding of galaxy formation. This is a further indication that such large values of the scatter in abundance matching are problematic.

function. To guide our choice, we consider that our primary goal in constructing mock catalogs is to reproduce the observational selection effects in the DEEP2 sample as accurately as possible. From that perspective, an inaccurate luminosity function is likely to be more damaging than an inaccurate two-point function, so we choose to prioritize the former over the latter. Only models with scatter below ~ 0.2 dex are then allowed. As shown in Figure 1, scatter values in this range have little to no significant impact on the clustering, so in the interest of simplicity in our modeling, we choose to implement a zero-scatter abundance matching model to construct DEEP2 mock catalogs.

Before we move on, however, it is worth exploring the impact that including scatter would have on the mocks we produce. Figure 3 shows the HODs that result from the various fixed-scatter abundance matching models we considered in the previous two figures, for two different luminosity thresholds. Solid lines show the overall HOD $\bar{N}(M)$, dashed lines show the HOD for central galaxies, $\bar{N}_c(M)$, and dotted lines show the HOD for satellites, $\bar{N}_s(M)$. The first thing to note is that, for scatter values above 0.2 dex, \bar{N}_c never reaches unity, implying that even some very massive halos do not host bright cen-

tral galaxies in these models. This occurs because, as mentioned above, the no-scatter luminosity function has become infinitely steep at the bright end, which is equivalent to the mean $L(v_{\max}^{\text{acc}})$ relation's becoming flat at high v_{\max}^{acc} . In that case, the large scatter will cause some central galaxies to scatter below the luminosity threshold of interest at all masses. This situation is strongly at odds with theories of galaxy formation, however and is another indication of the problematic nature of these high-scatter models.

For the models with scatter of 0.2 dex and below, the HODs are more well behaved, and we note that the impact of the scatter occurs mainly at low masses, softening the cutoff in \bar{N} but having little impact on the form of the HOD at large masses. We expect that a more accurate, variable-scatter abundance matching model would increase the scatter in luminosity at low subhalo masses, while keeping the scatter small at high masses. This would be expected to further soften the low-mass cutoff, while having similarly little impact on the power-law part of the HOD at high masses. Thus, we anticipate that the galaxy mass-selection function we infer from our final mock catalogs in this work will be somewhat steeper in mass than occurs in the real universe. However, the mocks should prove reasonably accurate above that mass threshold, and in particular they should give an accurate representation of the galaxy occupation of massive groups and clusters, at least for the bright galaxies observed by DEEP2, making them appropriate for use in optimizing cluster-detection algorithms. We explore their use for that purpose in Gerke et al. (2012). We also note in concluding this section that, should a more accurate, variable-scatter modeling approach be developed in the future, it could straightforwardly be combined with the techniques we develop below to assign galaxy colors and produce realistic DEEP2 mock catalogs that account for all observational selection effects.

3.2.3. Populating the lightcones with an evolving DEEP2 luminosity function

To produce the galaxy luminosities in our mock lightcones, then, we will abundance match the v_{\max}^{acc} function of halos and subhalos to the DEEP2 luminosity function, with zero scatter in the resulting $L(v_{\max}^{\text{acc}})$ relation. This is complicated somewhat by the broad redshift range covered by DEEP2, over which the luminosity function undergoes significant evolution (*e.g.*, W06, Faber et al. 2007). Fortunately, this evolution is consistent with simple luminosity evolution of the global galaxy population, with no overall evolution in number density or luminosity-function shape. Therefore, we can reproduce the DEEP2 luminosity function by performing abundance matching with a single luminosity function, measured at a particular redshift z_0 in DEEP2, and then applying a redshift-dependent correction to the luminosities of the mock galaxies.

Faber et al. (2007) found that the evolution of the overall DEEP2 luminosity function was reasonably well described by a pure linear brightening of M_B^* by 1.2 magnitudes per unit increase in redshift. However, redshift is not particularly well motivated physically as a parameter against which to measure galaxy evolution. We have thus reconsidered the measured M_B^* data points from Faber et al. (2007) as a function of the cosmic scale fac-

tor $a = 1/(1+z)$. A linear fit to the scale factor yields a better description of the data than a linear fit to redshift; therefore, in constructing the DEEP2 mocks we will implement an evolving M_B^* that dims by 2.45 magnitudes per unit increase in a .

More exactly, we populate the mock DEEP2 lightcones using an evolving luminosity function that takes the Schechter (1976) form,

$$\phi(M) = 0.4 \ln(10) \phi^* 10^{0.4(M^*(a)-M)(1-\alpha)} \times \exp(-10^{0.4M^*(a)-M}), \quad (1)$$

with

$$M^*(a) = M^*(a_0) + Q_a(a - a_0) \quad (2)$$

and $a_0 = (1+z_0)^{-1}$. The parameters we use are listed in Table 2. They are based on the DEEP2 values measured at $z \sim 0.9$ in W06, with a few modifications. First, the value for M_B^* is shifted brighter by 0.13 magnitudes to be consistent with the best fit to the evolution of $M_B^*(a)$. Second, because the measured value of ϕ^* at $z = 0.9$ is the highest measured value in all of DEEP2, we instead take the mean of all values measured at $z > 0.7$ in DEEP2, which lowers ϕ^* from the $z = 0.9$ value by about 12%.

Finally, we also correct this value of ϕ^* to account for the different cosmological background models in each of our three N-body simulations. W06 assumed a Λ CDM cosmology with $\Omega_M = 0.3$ in their measurements, using a volume element computed in that cosmology to convert the redshift-space galaxy counts to a number density. Since they would have inferred a different number density had they assumed the cosmology in each of our simulation boxes, we must correct the measured value of ϕ^* by a factor $V_{0.3}/V_{\Omega_M}$, where the volume is given in terms of the comoving line-of-sight distance $r(z)$ as

$$V_{\Omega_M} = 4\pi \int_{0.8}^{1.0} r^2(z) \frac{dr}{dz} dz, \quad (3)$$

$V_{0.3}$ is the value for $\Omega_M = 0.3$, and the integral is taken over the redshift range considered for the $z \sim 0.9$ measurement of the DEEP2 luminosity function in W06. The comoving distance is given by the usual Λ CDM equation

$$\frac{dr}{dz} = \frac{c}{H_0 \sqrt{\Omega_\Lambda + \Omega_M(1+z)^3}}. \quad (4)$$

The procedure we have outlined here ensures, by construction, that the luminosity function of our DEEP2 mock catalogs will match the input luminosity function to within Poisson noise. Figure 4 shows the comparison in bins of redshift. Data points are the measured luminosity function for all 40 of the Bolshoi lightcones, solid lines are the curves corresponding to the measured parameters from DEEP2 in W06, and dotted lines are curves corresponding to Equation 2 for the parameters given in Table 2. The dropoff in the low-luminosity datapoints at high redshift occurs because of an evolving luminosity cut we apply to the catalog, which excludes galaxies that are obviously below the DEEP2 apparent magnitude limit, to keep the catalog sizes manageable. Apart from this, the agreement between the luminosity function in the mocks and the input model is perfect, as expected.

Table 2
Parameters of the evolving luminosity function used to produce the mock lightcones.

| Parameter | Value |
|----------------------|-----------------------|
| $M_B^* - 5 \log h^a$ | -20.8 |
| ϕ_B^{*b} | 7.90×10^{-3} |
| α | 1.30 |
| Q_a | 2.45 |
| z_0 | 0.90 |

^a AB magnitudes.

^b In comoving $h^3 \text{ Mpc}^{-3}$, for a ΛCDM cosmology with $\Omega_M = 0.27$. This value is corrected to correspond to account for the different volume-redshift relation in each mock cosmology.

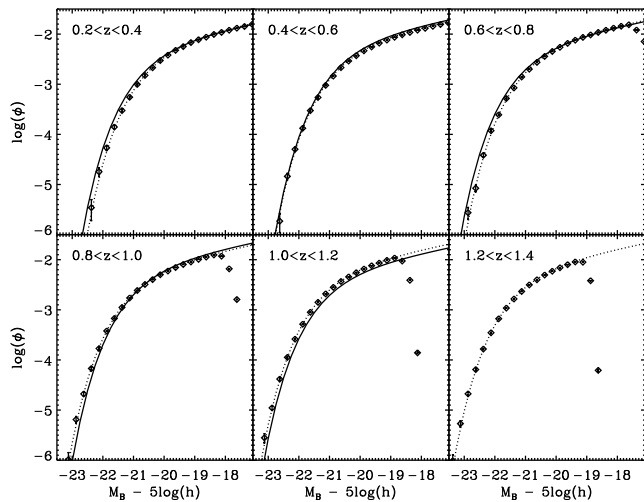


Figure 4. Comparison of the DEEP2 luminosity function to the luminosity function in the mock catalogs. Solid lines are the DEEP2 luminosity function as measured in W06. Dotted lines are the evolving luminosity function as parameterized in Table 2, which was used as an input to the mock-catalog creation algorithm. Data points are the measured number density of galaxies in the mock, in bins of luminosity, with units of $h^3 \text{ Mpc}^{-3} \text{ mag}^{-1}$ and Poisson error bars.

3.3. Color assignment by environment matching

Accurately reproducing the luminosity function, though necessary, is not sufficient to fully model the DEEP2 galaxy selection function. As discussed at length in, *e.g.*, W06 and Gerke et al. (2007), DEEP2’s $R = 24.1$ apparent magnitude limit translates into a B -band limit at $z \sim 0.75$ and a U -band limit at $z > 1$. This means that, at a given luminosity, red galaxies will drop out of the DEEP2 sample at a lower redshift than blue galaxies. There is a well-known strong correlation between galaxy color and galaxy environment, *i.e.*, local galaxy density (*e.g.* Hogg et al. 2004), and this relation persists to $z > 1$ in DEEP2 (Cooper et al. 2006), although it evolves strongly with redshift (Cooper et al. 2007; Gerke et al. 2007). If we are to use our mock catalogs for applications that probe the galaxy density field, such as testing and calibrating cluster-finding algorithms, it is important to include the effects of color-dependent selection on the

spatial sampling of galaxies. This will require that we accurately reproduce the color-environment relation.

Kitzbichler & White (2007) used a semi-analytic model for galaxy formation (from Croton et al. 2006, as updated by De Lucia & Blaizot 2007), in an effort to reproduce such effects in their mock catalogs. Unfortunately, this model does not accurately reproduce the color-magnitude-environment relation that is present in DEEP2 at $z \sim 1$; in particular, it produces too few faint, red galaxies in dense regions. This is a common feature of most semi-analytic models at present, and it likely to be a particular problem for using these mocks to test group-finding algorithms, since the number of observed galaxies in real groups will be lower than is predicted by the semi-analytic model.

Fortunately, the existence of an empirical color-density relation for galaxies also suggests a purely empirical means for reproducing it in mock catalogs, if our goal is simply to reproduce the features of the data, without necessarily understanding the astrophysical processes necessary to produce them in detail. Just as we were able to populate the N-body simulation with galaxy luminosities by making use of the known relation between luminosity and halo mass, we can add galaxy colors using the relation between color and local galaxy density. This will be slightly more complicated than the approach we used to add luminosities, since in that case we were able to posit a very tight (indeed, zero-scatter) relation between mass and luminosity, whereas the measured color-density relation in DEEP2 has an extremely large scatter (Cooper et al. 2006), within which the galaxy colors take their usual bi-modal distribution between red and blue objects. Furthermore, there is also a strong correlation between galaxy color and luminosity (and thus presumably also between color and mass¹⁰) via the well-known red and blue sequences, and each of these correlations may be evolving with redshift.

To ensure that we accurately capture the correlations between color, luminosity, and galaxy environment, and the scatter and evolution in these relations, we use a procedure that can be briefly outlined as follows. First, we divide both the DEEP2 dataset and the mock catalog into bins of redshift, luminosity, and local galaxy density. Within each bin, we select galaxies at random from DEEP2 (with replacement, and after applying a weighting to account for the color-dependent DEEP2 redshift-failure rate). For each galaxy thus selected, we assign its k -corrected $U - B$ color (as computed in W06) to one of the galaxies from the same bin in the mock. We explain each step in this procedure in more detail below. Our approach automatically reproduces the measured color distribution from DEEP2 in each bin and therefore also the evolving color-luminosity-density relation and its scatter. It is inspired by the ADDGALS algorithm (Wechsler et al. in preparation) that was used to produce mock catalogs for use with the Sloan Digital Sky Survey cluster-finding efforts (*e.g.*

¹⁰ Indeed, there is much debate in the literature at present regarding the relative importance of halo mass and local environment in determining galaxy color, with a large contingent arguing that mass is the more fundamental parameter (*e.g.*, Woo et al. 2012). For our purposes, though, it is sufficient to note that these correlations exist in the data, whatever their underlying cause, and attempt to reproduce them in the mocks.

Koester et al. 2007b; Johnston et al. 2007; Rozo et al. 2007) and several other purposes, including testing photometric redshifts (Gerdes et al. 2010) and spectroscopic followup (Cunha et al. 2012). Our algorithm differs from ADDGALS, however, in its use of subhalo abundance matching to assign luminosities and in various details of the color-assignment algorithm—e.g., the use of broadband colors, rather than SEDs—that make it specific to DEEP2 mock-making.

3.3.1. Choosing an environment measure

We have not yet specified what metric we will use to measure local galaxy density in this process. Cooper et al. (2005) tested a number of different possible density measures in the YWC catalogs and found that the distance to the n th-nearest neighbor reproduced the underlying galaxy density field with the best combination of fidelity and dynamic range. The basic strategy is to compute the projected distance r_n to the n th-nearest neighbor within a window of $\pm 1500 \text{ km s}^{-1}$ in the redshift direction. This can then be converted into a surface-density measure,

$$\Sigma_n = n / (\pi r_n^2). \quad (5)$$

Because the mean density of a magnitude-limited galaxy sample falls with redshift, it is also important to normalize the density to account for this; we can do this by converting the density values to *overdensities*,

$$\delta_n = \Sigma_n / \langle \Sigma_n(z) \rangle, \quad (6)$$

where the quantity in the denominator is the smoothed mean density computed in rolling bins of redshift. This measure is convenient for our purposes since it is the one that was used to measure the color-environment relation and its evolution in DEEP2 (Cooper et al. 2006, 2007). In this work we will follow those studies and measure local galaxy density in DEEP2 by computing the third-nearest neighbor overdensity δ_3 , since $n = 3$ was the value that Cooper et al. (2005) identified as giving the most accurate measure of local density in DEEP2.

Because the DEEP2 targeting algorithm can only schedule $\sim 70\%$ of appropriate targets for spectroscopy, and because the redshift-success rate is $\sim 70\%$, the overall sampling rate of the magnitude-limited pool of DEEP2 targets is $\lesssim 50\%$. When estimating the local environment in the mocks for color assignment, we are considering a complete, volume-limited sample, so the third-nearest-neighbor distance will probe the density field on smaller scales in the mocks than it will in DEEP2. It will be preferable to choose a density estimator in the mocks that is comparable to the δ_3 values that would be measured after accounting for all observational effects. To find the appropriate estimator, we computed various n th-nearest-neighbor overdensities within an early version of these mock catalogs. We then applied the DEEP2 targeting algorithm and a simple redshift-failure rate (see the following sections for details), and we computed the DEEP2 estimator δ_3 for the resulting “observed” catalog. A comparison of the various density measures showed that the projected *seventh*-nearest-neighbor overdensity in the volume-limited mock δ_7 was most tightly correlated with the as-observed δ_3 values. Therefore we will use δ_7 as our density estimator for color assignment in the mocks.

A possible complication is that, even if δ_3 and δ_7 are strongly correlated, their absolute values may not be directly comparable. It is not guaranteed that the correlation will lie along the line of equality on a plot of δ_3 versus δ_7 . One might suppose, for example, that the maximum overdensity in the sparsely sampled DEEP2 catalog might have a lower numerical value than the maximum in the volume-limited catalog. Thus, simply binning the data in δ_3 and the mock in δ_7 may not give comparable samples in corresponding bins. To deal with this, we divide each catalog into quintiles of local density and assume that corresponding quintiles of measured overdensity contain galaxies with comparable physical local densities. For example, the most overdense 20% of mock galaxies receive colors drawn from the most overdense 20% of DEEP2 systems, and so on.

A final concern for computing projected nearest-neighbor distances is edge effects. If a galaxy lies close enough to the edge of a field that its true n th-nearest neighbor lies outside the field, then the measured δ_n for that galaxy will be misestimated. This problem can be handled straightforwardly by imposing buffer regions near the field edges. In the DEEP2 data, we exclude from our color-assignment algorithm all galaxies that lie within 1 comoving h^{-1} Mpc from any edge or gap in the observed region. This ensures that only galaxies with accurately measured δ_3 values are used to assign colors. In the mocks, we would like to assign colors to all galaxies within the observed region, so we cannot perform the same exclusion. Instead, we construct our mock light-cones to have an angular extent that is larger than a DEEP2 observed field by 0.2 degrees in either direction. This creates an 0.1 degree buffer all the way around the “observed” region of the mock, so that galaxies in that area will have accurately measured values of δ_7 .

3.3.2. Adding colors to the mock galaxies

Having specified our mapping between overdensity measured in DEEP2 and in the complete, volume-limited mock, we can proceed to add colors to the mock galaxies. Figure 5 gives a schematic picture of our color-assignment technique. Within a single bin of redshift and M_B ¹¹, we divide the DEEP2 sample into quintiles of δ_3 and the mock into quintiles of δ_7 . We then draw galaxy colors randomly from the galaxies in each DEEP2 quintile in turn, and we assign them to the galaxies in the corresponding mock quintile until all mock galaxies have been assigned colors. Because the DEEP2 redshift-success rate depends on color, before performing the random draw, we also weight the data by the incompleteness-correction weights computed in W06. (In the EGS field, we also divide out the color-dependent weighting that was applied in the DEEP2 target-selection algorithm for this field, to ensure that we have an unbiased color distribution.)

This approach can be applied straightforwardly in bins of redshift and M_B that are completely sampled by the DEEP2 survey. Within each redshift bin, however, there is a color-dependent threshold luminosity, below which DEEP2 constitutes a partially incomplete sample and

¹¹ A detail: our magnitude binning is performed after subtracting off the evolution of M_B^* with scale factor a ; that is, we construct bins of L/L^* .

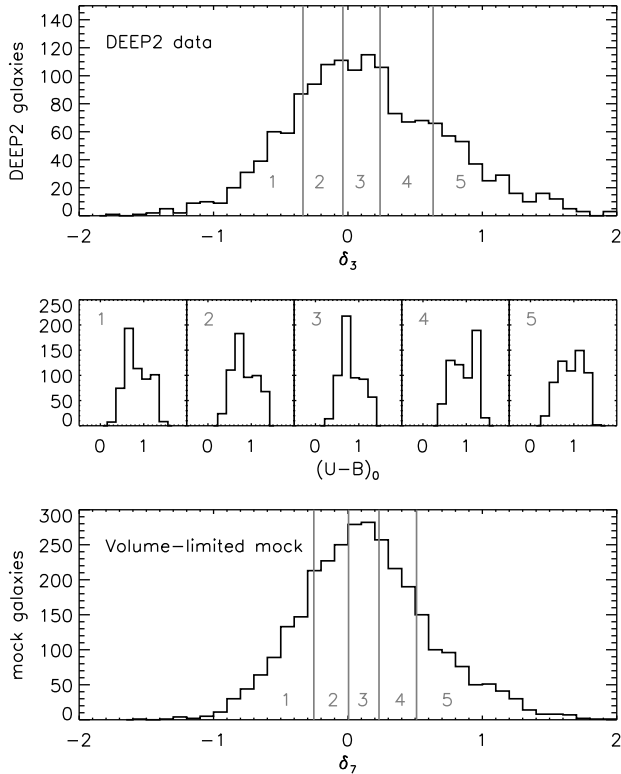


Figure 5. Schematic representation of our basic algorithm for adding galaxy colors to the volume-limited mock catalogs. Within a bin of redshift and absolute magnitude ($0.8 \leq z < 0.9$ and $-21 \leq M_B - 5 \log h < -20$ is shown here), we divide the DEEP2 data into five bins of local density δ_3 , containing equal number of galaxies. These bins are denoted by gray lines and numbers in the top panel. We divide the mock galaxies similarly into quintiles of δ_7 (bottom panel). We then assign rest-frame $U-B$ colors to the mock galaxies in each density quintile according to the color distribution in each of the corresponding DEEP2 density quintiles, after weighting these distributions to account for the color-dependent redshift failure rate (middle panels).

a minimum luminosity below which no DEEP2 galaxies are observed. Examples of these limits are shown in Figure 6. Because the DEEP2 R -band selection is performed in increasingly blue rest-frame bands as redshift increases, the bias against faint red galaxies also worsens. To determine whether we are working in a partially incomplete bin while assigning colors, in each bin we first perform a test color assignment on a fraction of the mock galaxies. We then compute R -band apparent magnitudes for this sample, as described in Section 3.3.3 below, and check for values that fall below the DEEP2 magnitude limit, $R = 24.1$. Assigning colors to mock galaxies in such bins will be more complicated than just described. To make this process easier, we work through the redshift and luminosity bins in increasing order of redshift and decreasing order of luminosity, to ensure that, for each partially incomplete bin, there is a nearby complete bin at lower redshift or brighter luminosity that has already been populated with mock colors.

In partially incomplete bins, it will be necessary to exclude some galaxies from the mock catalog by assigning them rest-frame colors that will put them below the DEEP2 apparent magnitude limit. We have no direct in-

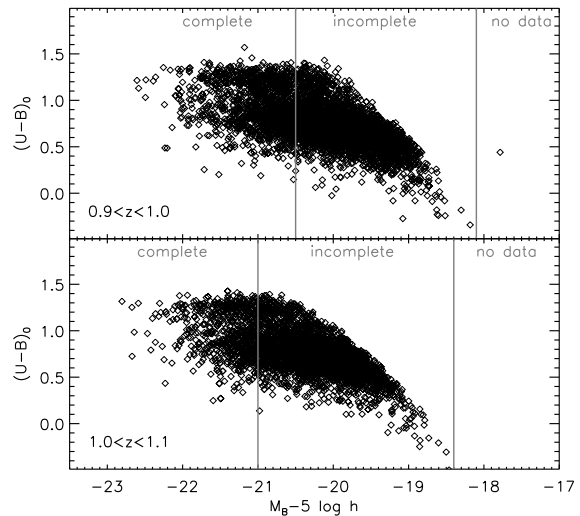


Figure 6. An illustration of redshift and color-dependent incompleteness in DEEP2. The panels show rest-frame color-magnitude diagrams for two different redshift bins, as computed using the k -corrections of W06. The sharp, tilted cutoff at the faint end corresponds to the DEEP2 $R = 24.1$ magnitude limit at the lower redshift limit of each bin. Vertical gray lines in each panel show the point at which the galaxy sample in each bin becomes partially incomplete (*i.e.*, some red galaxies start to drop below the magnitude limit at the highest redshifts in the bin) and the point at which all galaxies are lost from the sample. (The very faint outlier in the upper panel is an example of a galaxy with an incorrectly identified redshift. Such objects are rare and are excluded by construction from our color-assignment algorithm.)

formation about the density distribution of galaxies below the magnitude limit, but because the incompleteness depends on color, it is likely that it also has some correlation with galaxy environment. Our task, then, is to determine (a) how many galaxies to exclude, (b) with what distribution in local density, and (c) what colors to assign them so that they drop out of the mock DEEP2 survey.

The first step is relatively simple. To get a rough estimate of the number of mock galaxies to discard, we can simply compare the number density, n_{mock} , of mock galaxies in the redshift-luminosity bin in question and compare it to the number density of DEEP2 galaxies in the same bin, n_{DEEP2} , after weighting the DEEP2 galaxies with the W06 incompleteness-correction weights (which account for targeting incompleteness and redshift failures, but not incompleteness owing to the apparent magnitude limit). However, one expects some field-to-field variance in the mock owing to sample variance and shot noise, and we would obviously like this variance to be reflected in the mocks. We can straightforwardly compute the impact of this scatter on a particular mock lightcone by integrating the input luminosity function (see Equation 2 and Table 2) over the luminosity range of the bin in question and comparing the result to the actual number density in the mock lightcone being considered. This gives the size of the deviation from the mean DEEP2 number density in that particular redshift bin of that particular lightcone. Then the target number density of observed mock objects in that bin is given by

$$n_{\text{targ}} = \frac{n_{\text{DEEP2}} n_{\text{mock}}}{\int_{L_{\text{min}}}^{L_{\text{max}}} \phi(L) dL}, \quad (7)$$

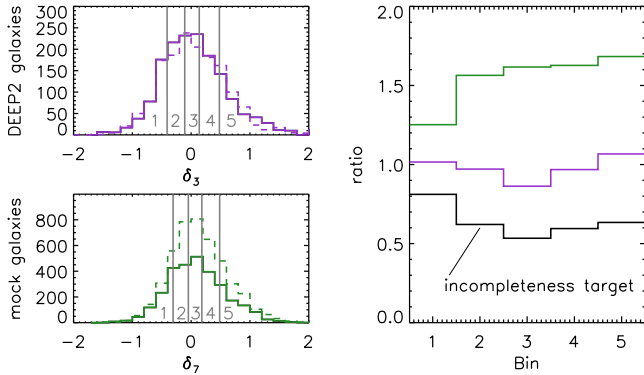


Figure 7. A schematic diagram showing our technique (described in detail in the text) for rejecting galaxies in a local-density-dependent way from bins of luminosity and redshift in which the DEEP2 sample is incomplete.

where L_{\min} and L_{\max} are the upper and lower limits of the luminosity bin being considered. Having computed this target number density, we can proceed to exclude galaxies from the mock until n_{targ} is reached.

Which galaxies should we exclude? It is extremely likely that the incompleteness in DEEP2 is a function of local environment, since it depends strongly on color, and it is important that we ensure that the overdensity distribution in the mocks is comparable to the one in the data before we perform color assignment. Since we cannot directly measure the overdensity distribution of unobserved DEEP2 galaxies, we will need to find some means of inferring it. Our approach is to make comparisons to the nearest complete bin at the same luminosity but lower redshift. The method is illustrated schematically in Figure 7. We start by dividing this lower redshift bin into quintiles of overdensity, both in the data and in the mock. Then, *holding the overdensity bins fixed*, we divide our incomplete bin into the same five bins of overdensity, in both the mock and the data. This is shown in the left-hand panels of the Figure, where the low and high-redshift bins are denoted by solid and dashed lines, respectively.

We then compare the ratios of the total number counts in each of the five overdensity bins (right-hand panel of the Figure). It is to be expected that the distribution of overdensity values in these bins will evolve in the mock catalog, owing to the evolution of cosmic structure (green curve). Because of density-dependent incompleteness, we expect that the distribution will appear to evolve differently in the data (violet curve). By taking the ratio of the relative change in the DEEP2 distribution to that in the mock (black curve), we can compute the number density of galaxies that ought to remain in the i th bin of overdensity after accounting for incompleteness:

$$\frac{n_{\text{targ}}^i(z)}{n_{\text{mock}}^i(z)} = \frac{n_{\text{DEEP2}}^i(z)}{n_{\text{DEEP2}}^i(z_0)} \left(\frac{n_{\text{mock}}^i(z)}{n_{\text{mock}}^i(z_0)} \right)^{-1} \frac{n_{\text{targ}}}{n_{\text{DEEP2}}} \quad (8)$$

where z_0 is the redshift of the nearest complete bin at this luminosity, and the final factor accounts for the expected sample variance in the mock lightcone in question (see Equation 7).

Having set these targets for the number density of mock galaxies in each bin of environment, we proceed to exclude galaxies from the sample using an iterative

process as follows. Using the overdensity binning that we established in the lower-redshift complete bin at z_0 , we assign provisional colors to the mock galaxies as described above, using the lower-redshift complete DEEP2 sample as the input sample. We then convert the mock galaxies colors and absolute magnitudes to apparent R -band magnitudes as described below. Since the bin we are considering is incomplete, some of these objects will have $R > 24.1$ and hence will drop out of the observed sample in the mock. For these galaxies, we retain the colors we just assigned¹² and exclude them from the sample; we erase the colors for the rest. We then repeat this procedure on the remaining galaxies until we have excluded enough galaxies to reach n_{targ}^i in this bin.

For the remaining mock galaxies in this bin, we then assign colors exactly as we did in the complete bins, by binning both the mock galaxies and the DEEP2 galaxies at the *current* redshift into quintiles of overdensity, then drawing DEEP2 colors at random from within each quintile to assign to the mock galaxies in the corresponding density bin. There is one small complication remaining, however. This bin has an incomplete region in color-magnitude space, and it is possible that some of the color assignments in the remaining mock galaxies will fall in this region. To guard against this, we test our color assignments by computing apparent R -band magnitudes as described below. For any galaxies with $R > 24.1$, we erase their colors and draw new ones, repeating this procedure until all the remaining mock galaxies have colors that place them above the DEEP2 magnitude limit. This completes the task of assigning colors to the mock in partially incomplete bins of redshift and luminosity.

For the faintest luminosity bins, where DEEP2 data is entirely lacking, or where there is no complete bin at lower redshift, we simply extrapolate from the color-density relation we used to populate the next-brightest bin, with one modification. Because galaxy luminosity and color are correlated, we shift the colors that we assign to the faint mock galaxies according to the mean relation, treating red galaxies and blue galaxies separately. First, we divide the DEEP2 sample into red and blue galaxies according to the division used by W06. We then fit for the mean linear color-magnitude relation of each of these samples separately, finding that red galaxies redden by 0.03 magnitudes per unit increase in absolute magnitude, while blue galaxies redden with a slope of 0.1 magnitudes. We use these relations to shift the assigned colors blueward, according to the difference in magnitude between the bright input galaxies and the faint mock galaxies that are having colors assigned. In this case, the input galaxies we use to assign colors are not DEEP2 galaxies but rather the galaxies in the next-brightest bin of the *mock*, since the DEEP2 sample will be incomplete, but this has been accounted for in the mock, as described above. (Thus, in this case, we use δ_7 as the density measure for both samples, but the algorithm is otherwise identical.) The color-density relation this produces is unconstrained by data and thus likely to be incorrect in detail, but this is irrelevant for any practical use of these mocks, and in any case the situation cannot be improved without more

¹² If the number of galaxies with $R > 24.1$ is larger than the number needed to reach n_{targ}^i , then we retain the colors for only faintest ones up to this number.

data.

3.3.3. Computing apparent magnitudes

Once we have assigned rest-frame B -band luminosities and $U - B$ colors to the mock galaxies, we can convert these to apparent R -band magnitudes m_R by empirically inverting the k -correction procedure that was used to compute the DEEP2 rest-frame values in W06. The rest-frame values are related to the observed magnitude by

$$m_R = M_B + D(z) - k, \quad (9)$$

where k , the k -correction, is a function of $U - B$ and z ; and $D(z)$ is the distance modulus. To obtain the appropriate k -correction for our mock galaxies, we infer it from the values computed for the DEEP2 sample as follows.

First, we divide the DEEP2 sample into narrow bins of width 0.01 in redshift. Within each of these bins, we fit a third-order polynomial to the relation between the k -corrections and the rest-frame $U - B$ colors that were computed in W06. As shown in the Appendix of that paper, $k(U - B)$ is a smooth, nearly linear function at fixed redshift, so our third-order polynomial fit will capture the relation well, and extrapolating a small distance into incomplete regions of color space will not be a problem. We use the fit thus obtained to compute m_R for each mock galaxy according to Equation 9. This technique is identical to the one used in Gerke et al. (2007) to compute observed magnitudes in the YWC mocks after assigning rest-frame colors in a manner similar to the one described above.

4. SIMULATING DEEP2 OBSERVATIONS

The mock DEEP2 lightcones we constructed in the previous section should fully capture the impact of the DEEP2 $R = 24.1$, but to fully characterize the DEEP2 selection it will also be necessary to account for the other observational effects present in the survey. These effects comprise the DEIMOS slitmask-making algorithm that schedules galaxies for spectroscopic observation; contamination by foreground stars and background galaxies; and the magnitude and color-dependent failure rate for obtaining reliable redshifts. We describe our methods for modeling each of these effects in turn below.

4.1. Mask-making: The DEEP2 targeting algorithm

DEIMOS is a multiplexed slit spectrometer, in which a custom-made mask is placed in the focal plane, with a slit cut in the position of each object that has been scheduled for observation. A number of practical constraints control the number of objects that can be observed in this manner. First, since the light is dispersed along a particular direction within the spectrograph, the slits must be oriented roughly parallel to an axis perpendicular to the spectral direction (within DEEP2 the slits are allowed to be tilted by up to 30 degrees from this axis). To avoid overlapping spectra on the detector, slits also may not overlap along this spatial axis. To allow for sufficient sampling of night-sky emission for sky subtraction, the slits must be long enough to allow empty regions of sky to be observed on either side of the target galaxies; this limits slit lengths to be no shorter than three arcseconds in DEEP2.

These limitations mean that galaxies in crowded regions on the sky will be less likely than average to be

assigned to a slit on a given mask. To mitigate the effects of slit-crowding, DEEP2 tiled the survey region with slitmasks in an overlapping pattern, so that nearly all galaxies have two or more opportunities to be assigned to a slitmask¹³. The DEEP2 slitmask creation algorithm is outlined in Davis, Gerke, & Newman (2004) and are described in detail by Newman et al. (2012).

The mock DEEP2 lightcones we described above are constructed to have an identical geometry to the three main DEEP2 fields, so the DEEP2 slitmask-making algorithm can be applied directly to the mocks to select mock galaxies for spectroscopic “observation” (though the mock lightcones must first be divided into three sub-cones, corresponding to the three photometric pointings making up each DEEP2 field).

The remaining complication is the pre-selection that is performed in observed BRI color-color space in the DEEP2 photometry. Since we have only produced observed R band apparent magnitudes, we cannot directly apply this selection to the mock catalog. The color-color pre-selection is tuned to select a nearly complete set of galaxies at $z \geq 0.75$, while excluding nearly all galaxies at $z \lesssim 0.7$ (Newman et al. 2012), so it should be possible to approximate it as a redshift-dependent selection weight. DEEP2 galaxies in the EGS were selected without this pre-selection, so we can use this field to test the efficacy of the color selection and convert it into a redshift selection. The EGS sample confirms that the DEEP2 color cuts are a highly efficient means of selecting high-redshift galaxies: only a few percent of $z > 0.75$ galaxies in the EGS are excluded by the cuts (and many of these have large photometric errors), while a large fraction of lower redshift objects are excluded. Apart from a small residual population of foreground galaxies (which we deal with below), the DEEP2 color pre-selection can be accurately approximated as a redshift-dependent selection probability as follows:

$$p_{\text{sel}}(z) = \left(1 + e^{-43.7(z-0.725)}\right)^{-1}. \quad (10)$$

We apply this selection probability to the mock galaxies before passing them through the DEEP2 slitmask making algorithm. We also exclude all galaxies with $z > 1.4$ in this selection step, since the [OII] $\lambda\lambda 3727$ doublet leaves the DEEP2 spectral window at this redshift, so the redshift success rate of DEEP2 galaxies drops dramatically at higher z . We will account for these higher redshift objects, as well as foreground objects and stars, below. This accurately reproduces the redshift distribution of DEEP2 in the range $0.7 \lesssim z \leq 1.4$, but it does not correctly account for the color dependence of the selection near the redshift cutoff. For this reason, the colors of “observed” galaxies in the main (non-EGS) DEEP2 mock catalogs presented here should be treated with caution at $z < 0.75$.

4.1.1. Foreground and background objects

The redshift selection function described above accurately captures the DEEP2 selection in the primary redshift range $0.75 \leq z \leq 1.4$. However, it does not account for the small but significant fraction of DEEP2

¹³ As discussed below, this increases to four chances in the EGS.

targets that do not lie in this range. These include objects in three categories: foreground ($z < 0.75$) galaxies that nevertheless pass the DEEP2 color pre-selection, foreground stars that have been misclassified as galaxies in the DEEP2 photometry, and background objects at $z > 1.4$. Since objects in each of these categories use up slit length that could otherwise be assigned to galaxies in the primary DEEP2 range, it is important to account for their effects on the DEEP2 slitmask-making algorithm. Since each of these samples is highly incomplete with complicated selection, it is nearly impossible to accurately reproduce the properties (*e.g.*, colors) of the objects in each set. Since such objects are not typically the focus of scientific analysis, and since we only wish to include their impact on the spectroscopic targeting, it is reasonable to include them in a random way as described below.

The sample of DEEP2 targets with reliable redshifts in the three non-EGS fields consists of roughly 1% stars and 4% galaxies at $z < 0.75$. Follow-up of the DEEP2 redshift failures with UV spectroscopy shows that an additional $\sim 15\%$ of DEEP2 targets lie at $z > 1.4$ (C. Steidel, private communication). To contaminate the sample with stars before applying the maskmaking algorithm, we draw R -band apparent magnitude values from a Gaussian distribution with mean 21.9 and dispersion of 1.5 magnitudes. We draw from this distribution and create potential spectroscopic targets (“stars”) at redshift zero in sufficient numbers to constitute 1% of the targets. To produce foreground and background galaxies, we select galaxies at random from the populations at $z < 0.75$ and $z > 1.4$ in appropriate proportions to match what is found in DEEP2, and we add these to the pool of potential spectroscopic targets. Once these contaminants are added to the mock catalog, we execute the DEEP2 slitmask making procedure on this sample, producing a list of objects that would be scheduled for DEIMOS observation in a real survey. This constitutes our mock DEEP2 spectroscopic sample.

4.2. Simulating redshift failure

Approximately 30% of DEEP2 spectroscopic targets do not yield good redshifts (Newman et al. 2012). As we mentioned above, roughly half of these lie in the so-called redshift desert at $z > 1.4$, where no strong galactic spectral features fall in the optical wavelength range. The remaining 15% fail to yield redshifts for a variety of reasons, most of which lead the observed spectrum to have a low signal to noise ratio. This redshift failure rate has some dependence on apparent magnitude and color: for example, faint red galaxies combine low flux with weak spectral absorption features, making them particularly susceptible to redshift failure. If we wish our mock catalogs to accurately model the selection function of galaxies with DEEP2 redshifts, it is important that we include color and magnitude dependence of redshift failure in our catalogs.

W06 developed a weighting scheme that accounts for color and magnitude-dependent incompleteness in DEEP2 by binning the spectroscopic targets in observed color-color-magnitude space and comparing the number of successful redshifts in each bin to the total number of photometric objects (making some justified assumptions about the redshift distribution of the spectroscopic tar-

gets that failed to yield a redshift). These weights can be straightforwardly inverted to yield an estimate of the redshift failure probability for a galaxy in a particular region of photometric space. To apply this probability to the mocks, when we assign rest-frame ($U - B$) colors to the mock galaxies by randomly drawing DEEP2 objects from within a bin of density, we also assign each DEEP2 galaxy’s incompleteness weight w_{corr} to the mock galaxy that receives its color.

We use the “optimal” set of weights from W06 for this purpose, with two small modifications. The weights account for incompleteness owing both to redshift failure and for targeting incompleteness (*i.e.*, the failure to schedule all suitable photometric objects for spectroscopy). Since we have already accounted for the latter type of incompleteness in the mock by running it through the DEEP2 slitmask-making algorithm, we must correct for this to avoid double-counting the targeting incompleteness. The slitmask-making algorithm does not depend on color or apparent magnitude, so the correction is simple: we need only multiply each weight by the fraction of potential targets that are scheduled for spectroscopic observation. (For galaxies in the EGS, it is also necessary to multiply out the redshift-dependent selection weighting described in the next section, which is straightforward.) In addition, there is a sharp drop in redshift success for the faintest 0.5 magnitudes of the DEEP2 sample (*i.e.*, galaxies with $23.6 \lesssim R < 24.1$). This is accounted for in the weighting scheme, but there is no guarantee that a mock galaxy will have exactly the same apparent R magnitude as the DEEP2 galaxy we used to assign its weight. Hence, if either the source DEEP2 galaxy or the target mock galaxy has $R > 23.6$, we apply a linear correction to the mock galaxy’s weight with a slope of 0.13 per unit magnitude difference between the target and source galaxy (applying a minimum of $R = 23.6$ on both galaxy magnitudes when computing the difference).

Each galaxy in the mock can then be assigned a probability of yielding a successful redshift, $p_z = w_{\text{corr}}^{-1}$, where w_{corr} is the W06 incompleteness weight, corrected for the targeting efficiency. We then use these probabilities to select stochastically a subsample of the spectroscopic targets that we declare to have “failed” redshifts, until the fraction of redshift failures (including both these stochastic failures and background objects at $z > 1.4$) matches the value in DEEP2. We will refer to the remaining targets as the “observed” mock galaxies. With this step, we have fully accounted for the color and magnitude-dependent DEEP2 selection effects in the mock catalogs, to the extent that it is possible to do so.

4.3. The Extended Groth Strip

In the EGS, spectroscopic targets are drawn from all regions of color-color space; no pre-selection is applied to exclude low-redshift galaxies. (However, as described below, the selection is *weighted* in color-color space, to stop the sample from being dominated by the more numerous low- z galaxies.) A sample that is magnitude-limited at $R = 24.1$ and extends to low redshift will include many nearby galaxies with very low-luminosity—and hence low mass. According to the W06 k -corrections, galaxies in the EGS have absolute magnitudes as low as $M_B \sim -11$, similar to the Leo dwarfs; the abundance-matching prescription we developed in Section 3.2 would place such

galaxies in halos with masses below $10^{10}M_{\odot}$. To include such low-mass halos in N-body models with cosmologically interesting volumes requires very high-resolution simulations, such as Bolshoi, which have only been computationally feasible within the last few years. The use of such simulations is one of the primary improvements of this work over the earlier mock catalogs of YWC04; it allows us to construct the first realistic mock catalog that includes the full range of redshift and luminosity probed by the EGS spectroscopic dataset.

When constructing the DEEP2 mock catalogs, we made use of data covering the full redshift range of EGS, $0 < z < 1.4$, making use only of data from the EGS at $z < 0.75$, where the primary DEEP2 spectroscopic sample is highly incomplete. Thus, our mock galaxies cover the full range of photometric and redshift space that is probed by DEEP2 spectroscopy in the EGS. However, there remain differences between the EGS dataset and the rest of DEEP2 that we must account for in constructing an EGS mock. The first is the field geometry and orientation. The three non-EGS DEEP2 fields are $0.5^{\circ} \times 2^{\circ}$ rectangular fields with their long axes oriented along lines of constant declination. The EGS, by contrast, is half as wide, at $0.25^{\circ} \times 2^{\circ}$, and is oriented perpendicular to the ecliptic, to allow easier access by space-based instruments. To account for these differences when constructing EGS mocks, we rotate the coordinate system of each of our mock lightcones to match the orientation of EGS and then excise the central 0.25° strip to use in EGS-like maskmaking. It is important to note that this approach means that our EGS lightcones are *not* independent from our main DEEP2 mocks; instead, each EGS cone corresponds exactly to one of the primary DEEP2 mocks.

The remaining differences between the EGS and the rest of DEEP2 involve the details of spectroscopic target selection. As we mentioned above, spectroscopic targets in the EGS are chosen from all regions of photometric color space, in contrast to the main DEEP2 sample, where a color pre-selection is applied. However, since a simple, magnitude-limited survey will always be dominated by the numerous fainter objects at low redshift, and since DEEP2’s primary goal is to explore the $z \sim 1$ universe, the EGS spectroscopic target selection is weighted in color space, so as to preferentially select high-redshift objects. The particulars of this weighting are discussed in detail by Newman et al. (2012). We briefly summarize it here. Galaxies in the EGS photometric sample are divided according to the same color pre-selection as is used in the primary DEEP2 fields. All galaxies that pass this selection cut (*i.e.*, the ones that would be observed in the rest of DEEP2), along with all galaxies brighter than $R = 21.5$, receive a uniform selection probability p_0 . For fainter galaxies that fail the selection cut in color space, the probability of spectroscopic observation is a function of flux, chosen so that roughly equal numbers of galaxies are observed above and below $z = 0.75$. This selection weighting is described in detail in Newman et al. (2012).

We apply this same probabilistic selection weighting in the spectroscopic targeting algorithm we use in constructing the EGS mocks, with the difference that the selection in color space is replaced with the selection in redshift given in Equation 10. The EGS targeting algorithm

also differs from the primary DEEP2 selection algorithm in its approach to tiling the observational area with slit-masks. Whereas the main DEEP2 survey strategy uses overlapping masks with a two-pass approach, the EGS targeting algorithm gives most galaxies *four* chances to be scheduled for observation, with one half of the masks oriented perpendicular to the other half, to further reduce crowding effects. We use an identical algorithm to “schedule” our mock EGS galaxies for spectroscopic observation. Then, after accounting for redshift failures as described in the previous section, we have a simulated DEEP2 EGS spectroscopic catalog that accounts for all major color and luminosity-dependent selection effects.

5. COMPARISONS TO DATA

Our aim is to produce mock catalogs by populating N-body models to reproduce various properties of the DEEP2 sample as accurately as possible. These include the luminosity function, luminosity-dependent two-point correlation function, color-magnitude diagram, and color-luminosity-environment relation—as well as the evolution of each of these with redshift. As discussed above, there is good reason to believe that reproducing these properties simultaneously will also correctly reproduce the underlying relation between luminosity, color, and dark-matter halo mass, thereby allowing the DEEP2 halo-mass selection function to be inferred.

In order to gauge our success in reproducing DEEP2 properties, it is obviously crucial to make direct comparisons to the data. This will also help to reveal any limitations of our mocks. We have already made comparisons above between our mock catalogs and the DEEP2 luminosity function (which our algorithm reproduces by construction; Figure 4) and the projected two-point correlation function (Figure 1) for different luminosity thresholds. Because of the evolving color-dependent selection cut imposed by the DEEP2 magnitude limit, it is also important to test the color, environment, and redshift properties of the mocks against the data as well. We make these comparisons in the remainder of this section. Throughout, we will use the Bolshoi mock catalogs as our basis for comparison to the data, since its background cosmology is in the best agreement with current constraints, but it will also be interesting to investigate the impact that different cosmological assumptions have in our three sets of mocks. We will conclude the section by briefly considering this issue.

5.1. The color-magnitude diagram

The first requirement for reproducing the DEEP2 color-dependent selection effects in our mocks is that we accurately reproduce the DEEP2 color distribution, its correlation with luminosity, and its redshift evolution. Figure 8 shows the rest-frame color-magnitude diagram for DEEP2 and the mock catalogs. For the mocks, both observed galaxies (black points) and unobserved galaxies (gray points) are shown. The qualitative features of the DEEP2 color-magnitude distribution are broadly reproduced in the mocks: distinct red and blue sequences are evident at all redshifts, with the correct loci in color-magnitude space and the correct color-magnitude correlations for observed galaxies; and the color-dependent selection cut in the mocks matches the one in the data

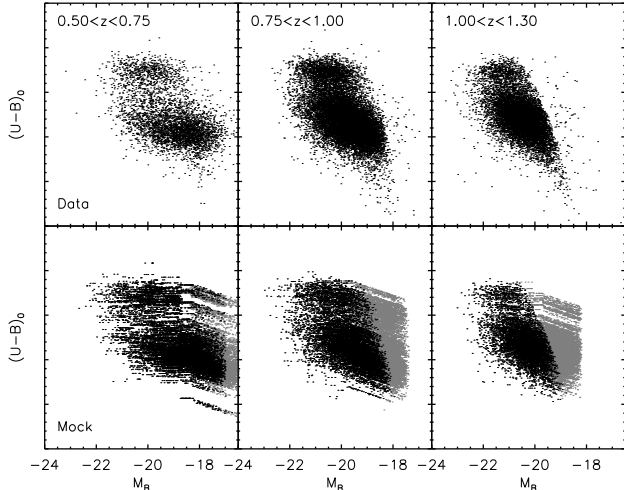


Figure 8. Comparison of the color-magnitude diagrams, in bins of redshift, for DEEP2 (upper row) and the mock catalogs presented here (lower rows). For the mock panels, black points show galaxies that were scheduled for observation and received a good redshift, while unobserved galaxies and redshift failures are shown in gray. The sources of the striping patterns visible in the mock panels are explained in the text.

(apart from a small number faint outliers in the data, which arise from incorrect redshift assignments).

Clear artifacts of our color-assignment process are evident in the mock diagrams, however, in the form of striping patterns. Two different kinds of stripe are apparent: horizontal stripes at bright magnitudes (especially at low redshift), and diagonal stripes for fainter objects. The latter stripes result from our method for assigning colors in luminosity bins where DEEP2 is incomplete, described in Section 3.3.2. In these bins, we have used the colors from brighter galaxies, shifted according to the mean color-magnitude relations for red and blue galaxies in DEEP2; the diagonal stripes for faint galaxies correspond to these relations. Horizontal striping occurs when the number of galaxies in a given DEEP2 luminosity-redshift bin is comparable to or smaller than the number of galaxies in the corresponding mock bin. This occurs especially at low redshift, since the EGS field has only half the area of the rest of the DEEP2 fields. For this reason, the low-redshift mock color-magnitude diagrams show a substantial striping and are extremely noisy.

We have not shown the $z < 0.5$ diagram in Figure 8, since this source of noise is so great there as to make comparison to the data uninformative. Since the comparison in the $0.5 < z \leq 0.75$ bin is not especially helpful either, for the remainder of this section we will focus on comparing the mocks with the high-redshift DEEP2 fields, excluding the EGS. If our techniques are successful at reproducing the high- z DEEP2 properties, then they should be equally successful in the EGS, within the confines of the limited data available in that region.

To allow a more quantitative comparison of the color and magnitude distributions, we plot histograms of apparent magnitude, absolute magnitude, and rest-frame color, over two different redshift ranges, in Figure 9. To make direct comparisons between the data and the mocks, we choose a subset of the 40 Bolshoi light cones with equal area to that covered by the high-redshift

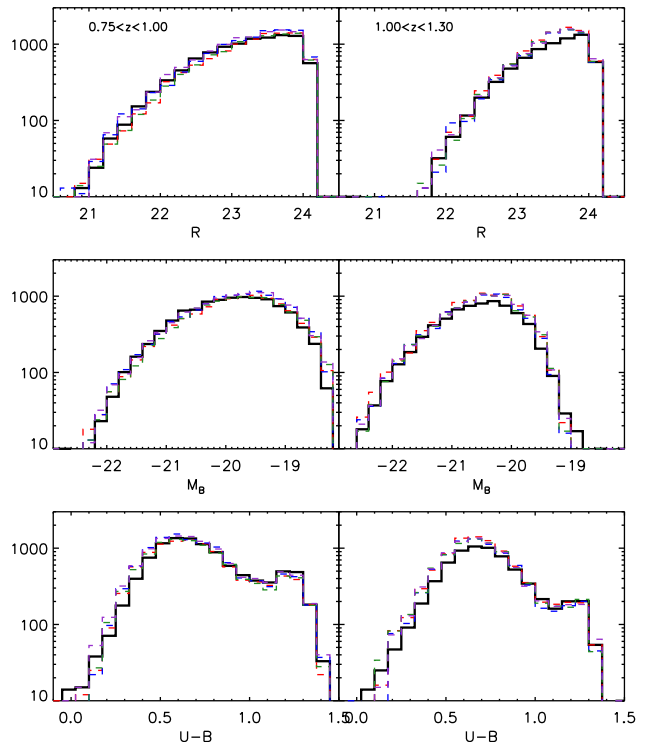


Figure 9. Comparison of the apparent and absolute magnitude and rest-frame color distributions for the DEEP2 sample in the three high-redshift fields (black solid curves) and for four different mock realizations of identical volume to those fields (colored dashed curves).

DEEP2 fields; this constitutes a single mock realization of the DEEP2 survey. The figure shows histograms for the DEEP2 data (black solid lines) and for the observed galaxies in four different mock realizations (colored dashed lines); the four realizations give a sense of the scatter in these distributions. The agreement is quite good in general, although there is a small but systematic overabundance of faint, blue galaxies, especially at higher redshifts.

There are two explanations for this. First, we have used the best fit to the evolving DEEP2 luminosity-function parameters to populate our mocks, rather than using the best fitting luminosity function at each redshift. This means that the mock luminosity function may lie above or below the DEEP2 one in a given redshift bin. As shown in Fig 4, the input luminosity function (dotted curve) lies above the best-fitting DEEP2 luminosity function in the $1.0 < z < 1.2$ bin. This explains why the high- z absolute magnitude distributions for the mocks lie systematically above the DEEP2 distribution, for example. However, the excess appears to be more significant at fainter magnitudes, and this faint-end excess persists in the low-redshift bin, where the input luminosity function matches the DEEP2 best fit more closely. This is likely explained by inaccuracy the faint-end slope of the input luminosity function. W06 held this parameter fixed at a value of 1.30, since DEEP2 does not extend to faint enough magnitudes for a robust fit, and we have adopted this value here (Table 2). Inspection of

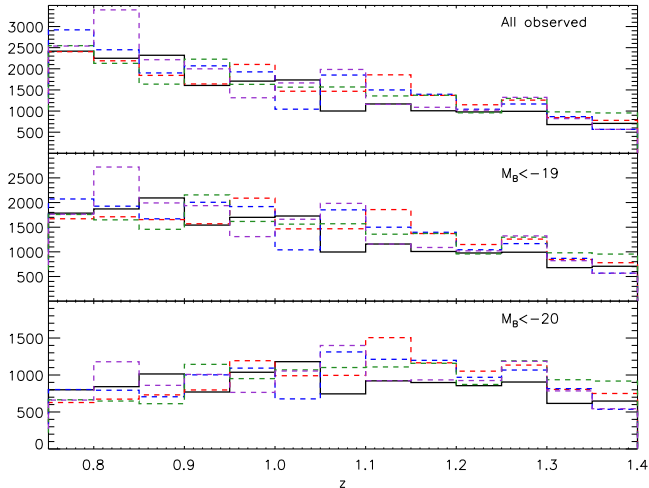


Figure 10. Comparison of the redshift histograms for the DEEP2 sample in the three high-redshift fields (black solid curves) and for four different mock realizations of identical volume to those fields (colored dashed curves). The mock realizations and their color coding are the same as was used in Fig 9. The panels show all observed galaxies (top), galaxies brighter than $M_B = -19$ (middle), and galaxies brighter than $M_B = -20$ (bottom).

Figure 7 of W07 suggests that this fixed faint-end slope may slightly overestimate the faint-galaxy abundance in DEEP2 at $z > 0.6$, so it is not too surprising that the mocks show a slight excess of faint objects. This excess translates into the systematic overabundance of blue galaxies that is also apparent in Figure 9, since all of the faintest galaxies in DEEP2 are blue galaxies.

5.2. The observed redshift distribution

Another test of the color and magnitude distribution in the mocks is to compare the redshift distribution in the mocks to the DEEP2 distribution. Reproducing the redshift distribution is not trivial: since the DEEP2 magnitude limit is a strong function of redshift and rest-frame color, an accurate redshift distribution requires accuracy in the overall galaxy abundance, color distribution, color-luminosity relation, and the evolution of each of these with redshift. This means that the redshift distribution is a strong test of our mock-making techniques. Figure 10 shows the redshift distribution for DEEP2 and for the same four mock realizations used above, for all observed galaxies, and for two different thresholds in luminosity. The agreement is quite good, considering the scatter between the different mock realizations, except for a small but systematic overabundance of galaxies over the range $1.05 < z < 1.3$. As explained in the previous section, this excess can be explained by the difference between our input luminosity function and the true best-fit DEEP2 luminosity function over this redshift range. It would be possible to improve the agreement here by using the true best-fit DEEP2 luminosity function in each redshift bin, but this would be at the expense of a smoothly evolving luminosity function and would likely create unphysical and undesirable jumps in the mock galaxy abundance at particular redshifts. We thus consider the current distribution to be the best that can be achieved with the available data.

5.3. The relation between color and environment

As we discussed in Section 3.3, if we are going to reliably infer the DEEP2 halo selection function, it is essential that our mock catalog accurately reproduce the relation between galaxy color and environment, as well as the redshift evolution of this relationship. We have attempted to ensure this by assigning colors to our mock galaxies as a function of the local galaxy overdensity. Our method for doing this relied on comparing density values measured in the magnitude-limited DEEP2 sample to values measured in the volume-limited mock, and so we matched the colors in bins of *relative* overdensity, using the δ_3 parameter in the data and δ_7 in the mock. There is no obvious guarantee that this will translate to a mock that matches the *absolute* color-density relation from DEEP2. It is important that we compare the color-environment relation in the observed mock with the DEEP2 data, to see how well the technique has worked.

This comparison is shown in Figure 11. The left panel shows the median third-nearest-neighbor galaxy overdensity δ_3 , in bins of rest-frame $U-B$ color, over the redshift range $0.8 < z < 1.0$. The black diamond points constitute an update to the results of Cooper et al. (2006) and show the DEEP2 color-density relation for the final DEEP2 galaxy sample. The red triangles show the same quantities for the mock catalogs, where δ_3 has been computed using only the observed mock galaxies (i.e., those that were targeted for observation and received a valid redshift). The agreement between the two samples is remarkable, especially given the large number of selection effects (apparent-magnitude limit, spectroscopic targeting, and color-dependent redshift failure) that were applied to the mock catalog after the initial color assignment was done. This figure constitutes a strong confirmation that our method for adding colors in quintiles of environment accurately reconstructs the DEEP2 color-environment relation. Although this figure shows only median values of δ_3 over a narrow redshift range, we have confirmed that the full δ_3 distributions have similar shapes and that similar results obtain for different redshift ranges.

Because the DEEP2 color-environment relation also evolves strongly with redshift (Cooper et al. 2007), it is also important that we capture this evolution in the mocks as well. The right-hand panel of the figure compares this evolution in the data and the mocks. The black curves are an update to Figure 6 of Cooper et al. (2007): they show the fraction of galaxies that are red in the most overdense and most underdense 20% of the DEEP2 sample, in sliding bins of redshift with width 0.1 (where red galaxies are defined by splitting the red and blue sequences as in W06). The red fraction of underdense galaxies is roughly constant with z , while the overdense red fraction evolves strongly, especially at $z > 1$, so that the two populations are nearly indistinguishable in terms of red fraction at $z = 1.3$. The red curves in the figure show the same quantities for the mocks; the same qualitative behavior is evident, and the agreement between the mocks and the data is quite good over the full redshift range considered.

The excellent agreement between the mocks and the DEEP2 data in terms of redshift, color, and color-density relation suggests that these mocks will be useful for exploring the impacts of DEEP2’s color, redshift, and density selection functions on the selection of dark matter

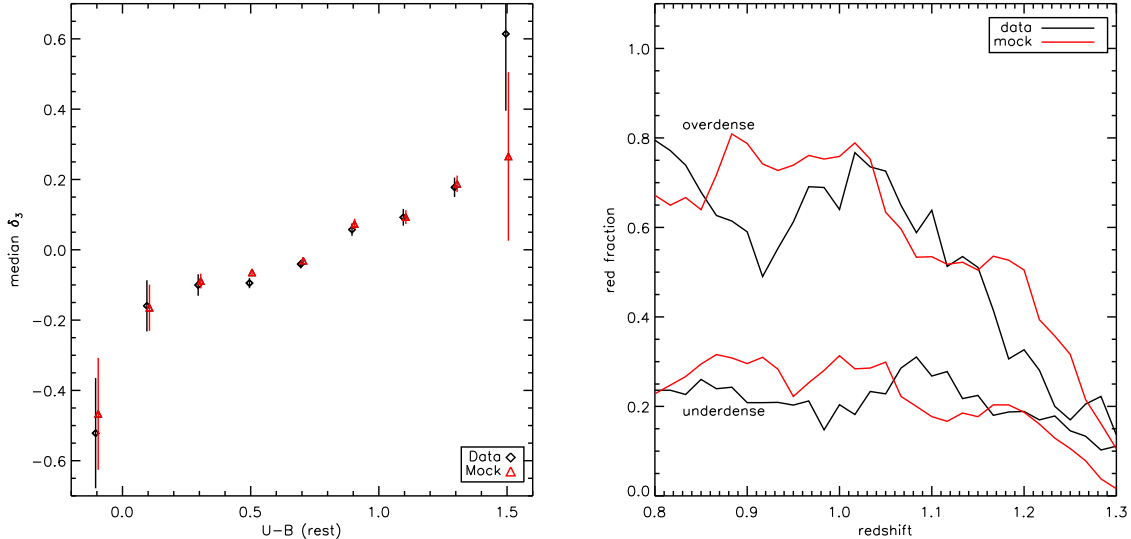


Figure 11. Comparison of the color-environment relation, and its redshift evolution, in DEEP2 and the mock catalogs. *Left:* The median value of the local overdensity parameter δ_3 is shown in bins of rest-frame color, for the DEEP2 data (black points) and the mock catalogs (red points). Error bars show the standard error, and points have been offset slightly in the horizontal direction for clarity. Here δ_3 in the mocks has been computed using only observed mock galaxies, as for DEEP2. *Right:* A comparison of the evolution of the color-density relation in the data and the mocks. Curves labeled *overdense* and *underdense* show the fraction of red galaxies for the most overdense and most underdense 20% of galaxies, respectively, where red galaxies are defined according to the red–blue division in W06. Black curves show the red fractions in DEEP2, and red curves show the values from the mock catalogs. Error bars on these curves are similar to the ones shown in Figure 6 of Cooper et al. (2007) and are much smaller than the difference seen between the samples at low z ; they are suppressed here for the sake of readability.

halos. The Appendix gives an example of how the mocks might be used for this purpose.

5.4. The Halo-occupation distribution and the impact of cosmology

Before we conclude, it will be interesting to explore the importance of the background cosmology on the accuracy of the mock catalog. Recall that we have constructed DEEP2 mocks for three different simulation boxes with three different cosmologies (listed in Table 1). Throughout all of the above comparisons, we have considered only the Bolshoi simulation, since its background cosmology is the most consistent with current cosmological constraints, and we have found that the Bolshoi mocks will be useful for probing the DEEP2 mass selection function at high halo masses. We would like to know the other mocks are likely to be similarly useful or not.

The most direct way to test this is to consider the HOD. Since the halo-occupation probability will feed directly into the inferred halo selection function, if this quantity depends strongly on cosmology it will be especially important to make sure our simulation box has a background cosmology that is consistent with existing constraints. If the dependence is weak, then this is less critical. We can compute the HOD for each of our mocks by dividing the dark matter halos into bins of mass and counting the mock galaxies in each halo above a given luminosity threshold, and then averaging these counts over the mass bin. It will also be interesting to compare these mock HODs to the HOD that Zheng, Coil, & Zehavi (2007) (hereafter ZCZ07) inferred from the DEEP2 clustering measurements. This will constitute another comparison of the mocks to the data, albeit a model-dependent one, since the inferred DEEP2 HOD makes assumptions about the background cosmology.

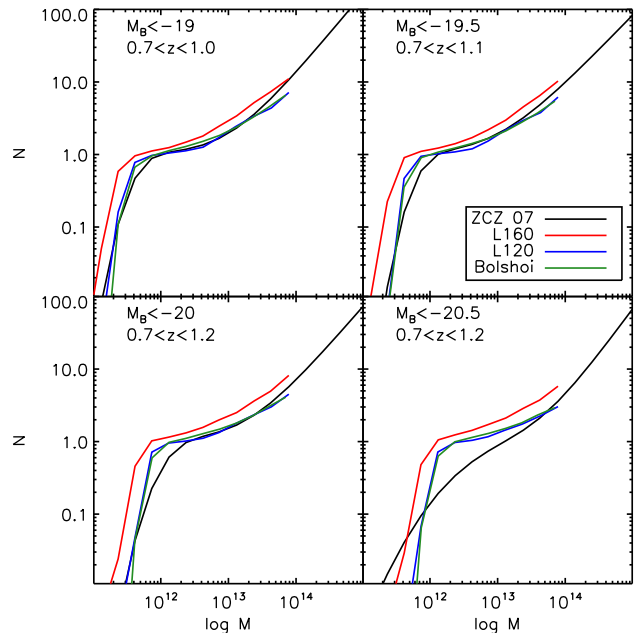


Figure 12. Halo occupation distributions for the three different mock cosmologies, with different luminosity thresholds, compared to the analogous HODs that Zheng, Coil, & Zehavi (2007) inferred for DEEP2. A clear dependence of the HOD on background cosmology (explained in detail in the text) is evident. The L120 and Bolshoi mocks agree reasonably well with the data in all but the brightest bin (where the inferred DEEP2 HOD, as discussed in the text, is highly uncertain and problematic).

ogy.

Figure 12 shows the comparison for the same four luminosity thresholds that were used in ZCZ07. There is a clear difference between the mock from the L160 sim-

ulation box and the other two boxes, with subtler differences between the L120 and Bolshoi mocks. The reason for these differences is easy to explain. The luminosity-assignment algorithm inserts a fixed luminosity function $\phi(L)$, regardless of the underlying halo mass function. Thus, if the overall mass function has a lower normalization, we must place more galaxies in halos of a given mass to reproduce the desired luminosity function. Hence, a simulation with a lower normalization for its halo mass function (e.g., lower Ω_M or σ_8) will necessarily have a higher mean halo occupation number $\langle N \rangle(M)$ at fixed $\phi(L)$. Conversely, because a galaxy of a given luminosity would reside in a lower-mass halo, clustering at fixed luminosity would be reduced. The opposite effect would obtain in a simulation with a higher normalization.

Thus, the L160 mock, with its relatively low value of σ_8 has a significantly higher HOD at all masses than the other mocks. The differences between the L120 and Bolshoi HODs are smaller because their cosmologies (see Table 1) lie near a degenerate curve in $\Omega_M - \sigma_8$ space; that is, there is little difference between their mass functions. It is worth noting, though, that the Bolshoi mock HOD lies systematically above the L120 one in the mass range $10^{12} \lesssim M \lesssim 10^{13}$, which is an important transition region between the central-dominated and satellite-dominated parts of the HOD. Because there is a clear dependence of the HOD on cosmology in these mocks, we recommend that the Bolshoi mocks be used for nearly all purposes, since the others may give inaccurate selection functions. However, we also make the L120 and L160 mocks available to the public, *e.g.*, for the purposes of testing cosmology dependence.

The Bolshoi and L120 mocks also agree reasonably well with the HODs inferred from DEEP2, for all but the brightest galaxy sample. Black curves show the HOD models from ZCZ07 that best fit¹⁴ the DEEP2 clustering measurements from Coil et al. (006b). This agreement is not surprising, since ZCZ07 assumed a background cosmology identical to the one used in the L120 simulation. For the three lower luminosity thresholds, the Bolshoi and L120 HODs lie slightly below the DEEP2 measurement at high mass, and they cut off somewhat less steeply at low mass. There is a strong degeneracy in the ZCZ07 HOD model, however, such that increasing the sharpness of the low-mass cutoff can be offset by lowering the high-mass slope while keeping the predicted autocorrelation function roughly constant, so an even better agreement is likely possible within the model uncertainties. Since our zero-scatter model effectively requires a sharp low-mass cutoff, it is also possible that a model with somewhat higher scatter would be in closer agreement with the ZCZ07 results.

In the panel with the brightest luminosity threshold, the agreement with the inferred DEEP2 HOD is quite poor. However, the ZCZ07 fit in this bin is poorly constrained and depends strongly on the corrections that were applied to account for small-scale effects from crowding on the DEEP2 slitmasks. Furthermore, the ZCZ07 curve shown there is unphysical (as

ZCZ07 discuss), since it formally implies that halos with $M = 2 \times 10^{11}$ contain more galaxies with $M_B < -20.5$ on average than they do galaxies with $M_B < -20$. We thus do not find the disagreement at bright magnitudes to be a particular cause for concern.

6. SUMMARY AND CONCLUSIONS

We have constructed three sets of mock catalogs for the DEEP2 Galaxy Redshift Survey, derived from three different N -body simulations with different background cosmologies. In doing this, we have striven to reproduce, as accurately as possible, the DEEP2 HOD, as well as all of the important galaxy properties that might have an impact on DEEP2 galaxy selection. Meeting these goals required us to develop new empirical techniques to assign colors to our mock galaxies based purely on the color-environment relation in the DEEP2 data, since physically motivated galaxy formation models tend not to reproduce this relation accurately at high redshift. With the release of this paper, we also release the mock catalogs for use by the general public. Instructions for downloading the mock catalogs and detailed information on their contents can be found in the Appendix, along with a specific example showing how these mocks might be useful for estimating DEEP2 selection effects as a function of halo mass.

Our mock-making technique assigns mock galaxies to the halos and subhalos in the dark-matter-only simulations by directly imposing the empirical properties of DEEP2 on the simulations. We start by stacking simulation snapshots from different timesteps to construct lightcones with the geometry of DEEP2 fields, which accurately reproduces the redshift evolution of cosmic structure. We then use the subhalo abundance matching technique to assign galaxy luminosities to the halos and subhalos in each lightcone. This technique posits a tight, monotonic relation between the mass of a halo and the luminosity of the galaxy it hosts (with the caveat that the masses of subhalos should be measured before they are accreted into their parent halos).

To assign galaxy colors in such a way as to reproduce their strong dependence on luminosity, redshift, and local environment, we bin the DEEP2 and mock galaxies in luminosity and redshift and further subdivide these bins into quintiles of local n th-nearest-neighbor overdensity. We then draw DEEP2 galaxies at random from these bins and assign them to the mock galaxies in the corresponding bin, taking care to account for incompleteness in the DEEP2 sample at faint magnitudes. Having produced mock galaxies with redshifts, luminosities, and colors, we can invert the k -correction technique of W06 to assign apparent R -band magnitudes to the mock galaxies. These allow us to apply the DEEP2 apparent magnitude limit to our mock sample. We can also apply a redshift-dependent selection that closely approximates the effect of the DEEP2 selection in color-color space. Given these mock DEEP2 targets, we can apply the DEEP2 spectroscopic target-selection algorithm to reproduce the spatial selection effects inherent to multiplexed slitmask spectroscopy. Finally, to account for observations that fail to yield a redshift, we exclude a fraction of the mock galaxies according to the color and magnitude-dependent redshift-failure rate of DEEP2 galaxies.

This mockmaking technique accounts for all major ob-

¹⁴ The one exception to this is the lowest luminosity bin. In that bin, the formal best fit lies in a region of parameter space that ZCZ07 excluded on physical grounds, so in this panel we show a curve that lies within the parameter uncertainties and that approximately reproduces the curve in Figure 1 of ZCZ07.

servational effects that pertain to DEEP2 galaxies. The resulting mocks accurately reproduce a wide array of properties of the DEEP2 catalog, including the luminosity function; the color, magnitude, and redshift distributions; the color-environment relation and its evolution; and the inferred DEEP2 HOD for massive halos, provided that the background cosmology of the simulation is in agreement with current constraints. This accuracy gives us confidence that our DEEP2 mock catalogs will allow us to infer the selection of DEEP2 galaxies with reasonable accuracy as a function of dark-matter-halo mass, as well as the relations between halo mass and galaxy properties.

In the process of constructing the mock catalogs, we obtained two results that are of general scientific interest beyond the area of mock-catalog creation. First, when assigning galaxy luminosities using abundance matching techniques, we tried various different assumptions about the scatter in the mass-luminosity relation and compared the resulting projected two-point correlation functions $w_p(r_p)$ to the DEEP2 measurement. We find that no model with fixed log-normal scatter (in luminosity at fixed mass) gives simulated $w_p(r_p)$ consistent with the clustering measured in DEEP2. This is broadly consistent with the results of Wetzel & White (2010), who require a large value of the scatter to achieve even approximate agreement with the DEEP2 clustering results. For reasons discussed in Section 3.2.2, we do not believe that these issues will create problems when using these mocks to optimize group-finding algorithms, although they should be used with care for purposes that involve understanding the selection of low-mass halos.

In addition, because we have constructed mock catalogs from three separate N-body simulations with different cosmological parameters, we can probe the cosmology dependence of our mock-making techniques. We find that the HODs in the different mock catalogs vary strongly with cosmology. This arises directly from the technique for luminosity assignment. Because abundance matching maps the observed galaxy luminosity function to the simulated halo mass function at fixed number density, if the mass function dn/dM in a given simulation has a lower normalization than the true mass function in the universe, then the HOD resulting from the galaxy assignment must have a higher normalization and lower mass cutoff to compensate. For cosmologies with nearly identical mass functions (e.g., points lying along the same degenerate curve in Ω_M - σ_8 space), however, the impact on the HOD will be relatively small.

Thus, it is important when constructing mock catalogs from N-body models to use a simulation whose assumed cosmology is in agreement with all existing constraints, to ensure the best possible accuracy in the resulting HOD. For most applications, we therefore recommend the mock catalogs we have constructed from the Bolshoi simulation, since it is consistent with the best cosmological constraints available. The mocks constructed from the L120 and L160 simulations are likely to be generally useful only for testing the impact of varying assumptions about cosmology on any conclusions drawn from the mocks.

Given that the Bolshoi mocks should accurately reproduce the DEEP2 halo selection function, an immediately interesting use to which we can put them is testing and

calibrating an algorithm for detecting groups and clusters of galaxies. We have used them for this purpose in Gerke et al. (2012).

ACKNOWLEDGMENTS

BFG and RHW were supported by the U.S. Department of Energy under contract number DE-AC03-76SF00515. MCC acknowledges the support of the Spitzer space telescope fellowship program. We thank Marc Davis, Jeff Newman, Carlos Frenk, and especially Michael Busha for fruitful conversations. We thank Anatoly Klypin and Joel Primack for providing access to the Bolshoi simulation, which was run on the Pleades machine at NASA Ames. We thank Jeremy Tinker for providing us with his code to compute $w_p(r_p)$ in a simulation box.

REFERENCES

- Behroozi, P. S., Conroy, C., & Wechsler, R. H. 2010, *ApJ*, 717, 379
- Behroozi, P. S., Wechsler, R. H., Wu, H.-Y., Busha, M. T., Klypin, A. A., & Primack, J. R. 2013, *ApJ*, 763, 18
- Blaizot, J., Wadadekar, Y., Guiderdoni, B., Colombi, S. T., Bertin, E., Bouchet, F. R., Devriendt, J. E. G., & Hatton, S. 2005, *MNRAS*, 360, 159–175
- Bryan, G. L., & Norman, M. L. 1998, *ApJ*, 495, 80
- Busha, M. T., Wechsler, R. H., Behroozi, P. S., Gerke, B. F., Klypin, A. A., & Primack, J. R. 2011, *ApJ*, 743, 117
- Coil, A. L., et al. 2006a, *ApJ*, 638, 668
- Coil, A. L., et al. 2006b, *ApJ*, 644, 671
- Coil, A. L., Newman, J. A., Kaiser, N., Davis, M., Ma, C.-P., Kocevski, D. D., & Koo, D. C. 2004, *ApJ*, 617, 765
- Conroy, C., Wechsler, R. H., & Kravtsov, A. V. 2006, *ApJ*, 647, 201–214
- Cooper, M. C., et al. 2006, *MNRAS*, 370, 198
- Cooper, M. C., et al. 2007, *MNRAS*, 376, 1445
- Cooper, M. C., Newman, J. A., Madgwick, D. S., Gerke, B. F., Yan, R., & Davis, M. 2005, *ApJ*, 634, 833
- Croton, D. J., et al. 2006, *MNRAS*, 365, 11
- Cunha, C. E., Huterer, D., Busha, M. T., & Wechsler, R. H. 2012, *MNRAS*, 423, 909–924
- Davis, M., et al. 2003, *Proc. SPIE*, 4834, 161
- Davis, M., et al. 2007, *ApJ*, 660, L1
- Davis, M., Gerke, B. F., & Newman, J. A. 2004, *astro-ph/0408344*
- De Lucia, G., & Blaizot, J. 2007, *MNRAS*, 375, 2
- Eke, V. R., et al. 2004, *MNRAS*, 348, 866
- Faber, S. M., et al. 2003, In *Instrument Design and Performance for Optical/Infrared Ground-based Telescopes*. Edited by Iye, Masanori; Moorwood, Alan F. M. *Proceedings of the SPIE*, Volume 4841, pp. 1657-1669 (2003)., M. Iye and A. F. M. Moorwood, eds., volume 4841 of *Presented at the Society of Photo-Optical Instrumentation Engineers (SPIE) Conference*, pp. 1657–1669
- Faber, S. M., Willmer, C. N. A., Wolf, C., Koo, D. C., Weiner, B. J., Newman, J. A., Im, M., Coil, A. L., Conroy, C., Cooper, M. C., Davis, M., Finkbeiner, D. P., Gerke, B. F., Gebhardt, K., Groth, E. J., Guhathakurta, P., Harker, J., Kaiser, N., Kassin, S., Kleinheinrich, M., Konidaris, N. P., Kron, R. G., Lin, L., Luppino, G., Madgwick, D. S., Meisenheimer, K., Noeske, K. G., Phillips, A. C., Sarajedini, V. L., Schiavon, R. P., Simard, L., Szalay, A. S., Vogt, N. P., & Yan, R. 2007, *ApJ*, 665, 265–294
- Gerdes, D. W., Sypniewski, A. J., McKay, T. A., Hao, J., Weis, M. R., Wechsler, R. H., & Busha, M. T. 2010, *ApJ*, 715, 823–832
- Gerke, B. F., et al. 2005, *ApJ*, 625, 6
- Gerke, B. F., et al. 2007, *MNRAS*, 376, 1425
- Gerke, B. F., et al. 2012, *ApJ*, 751, 50
- Henriques, B. M. B., White, S. D. M., Lemson, G., Thomas, P. A., Guo, Q., Marleau, G.-D., & Overzier, R. A. 2012, *MNRAS*, p. 2442
- Hogg, D. W., et al. 2004, *ApJ*, 601, L29

- Johnston, D. E., Sheldon, E. S., Wechsler, R. H., Rozo, E., Koester, B. P., Frieman, J. A., McKay, T. A., Evrard, A. E., Becker, M. R., & Annis, J. 2007, arXiv:0709.1159
- Kitzbichler, M. G., & White, S. D. M. 2007, MNRAS, 376, 2
- Klypin, A., & Holtzman, J. 1997, arXiv:astro-ph/9712217
- Klypin, A. A., Trujillo-Gomez, S., & Primack, J. 2011, ApJ, 740, 102
- Knebe, A., Knollmann, S. R., Muldrew, S. I., Pearce, F. R., Aragon-Calvo, M. A., Ascasibar, Y., Behroozi, P. S., Ceverino, D., Colombi, S., Diemand, J., Dolag, K., Falck, B. L., Fasel, P., Gardner, J., Gottlöber, S., Hsu, C.-H., Iannuzzi, F., Klypin, A., Lukić, Z., Maciejewski, M., McBride, C., Neyrinck, M. C., Planelles, S., Potter, D., Quilis, V., Rasera, Y., Read, J. I., Ricker, P. M., Roy, F., Springel, V., Stadel, J., Stinson, G., Sutter, P. M., Turchaninov, V., Tweed, D., Yepes, G., & Zemp, M. 2011, MNRAS, 415, 2293–2318
- Koester, B. P., et al. 2007a, ApJ, 660, 221
- Koester, B. P., et al. 2007b, ApJ, 660, 239
- Kravtsov, A. V., Klypin, A. A., & Khokhlov, A. M. 1997, ApJ, 111, 73
- Kravtsov, A. V., Berlind, A. A., Wechsler, R. H., Klypin, A. A., Gottlöber, S., Allgood, B., & Primack, J. R. 2004, ApJ, 609, 35–49
- Le Fèvre, O., et al. 2005, A&A, 439, 845–862
- Lilly, S. J., et al. 2009, ApJS, 184, 218–229
- Muldrew, S. I., Pearce, F. R., & Power, C. 2011, MNRAS, 410, 2617–2624
- Newman, J. A., et al. 2012, ApJ, submitted, arxiv:1203.3192
- Peacock, J. A., & Smith, R. E. 2000, MNRAS, 318, 1144
- Reddick, R. M., Wechsler, R. H., Tinker, J. L., & Behroozi, P. S. 2013, ApJ, in press; arXiv:1207.2160
- Rozo, E., Wechsler, R. H., Koester, B. P., Evrard, A. E., & McKay, T. A. 2007, ArXiv Astrophysics e-prints
- Schechter, P. 1976, ApJ, 203, 297–306
- Tasitsiomi, A., Kravtsov, A. V., Wechsler, R. H., & Primack, J. R. 2004, ApJ, 614, 533–546
- Trujillo-Gomez, S., Klypin, A., Primack, J., & Romanowsky, A. J. 2011, ApJ, 742, 16
- Vale, A., & Ostriker, J. P. 2004, MNRAS, 353, 189–200
- Wetzel, A. R., & White, M. 2010, MNRAS, 403, 1072
- Willmer, C. N. A., et al. 2006, ApJ, 647, 853
- Woo, J., Dekel, A., Faber, S. M., Noeske, K., Koo, D. C., Gerke, B. F., Cooper, M. C., Salim, S., Dutton, A. A., Newman, J., Weiner, B. J., Bundy, K., Willmer, C. N. A., Davis, M., & Yan, R. 2012, MNRAS, submitted, arXiv:1203.1625
- Yan, R., White, M., & Coil, A. L. 2004, ApJ, 607, 739
- Yang, X., Mo, H. J., & van den Bosch, F. C. 2003, MNRAS, 339, 1057–1080
- York, D. G., et al. 2000, AJ, 120, 1579
- Zheng, Z., et al. 2005, ApJ, 633, 791–809
- Zheng, Z., Coil, A. L., & Zehavi, I. 2007, ApJ, 667, 760

APPENDIX

THE PUBLIC CATALOGS AND EXAMPLE APPLICATIONS

With the publication of this paper, we also release our DEEP2 mock catalogs for use by the general public. Mocks for each of the three different simulation boxes listed in Table 1 can be obtained as binary data tables in FITS format from the World Wide Web at <http://www.slac.stanford.edu/~risa/deepmocks>. In this section we describe the contents of the electronic mock catalog files and give a few examples of applications for which they might be useful.

The catalogs

We provide two sets of forty lightcones from the Bolshoi simulation, each of which has the geometry of a single DEEP2 field, with an additional buffer region around the edge of the field on the sky. One set of lightcones is selected to reproduce the primary (high-redshift) DEEP2 fields, and the other is selected to replicate the EGS. The dark-matter halo populations of corresponding lightcones in the two sets of mocks are identical. For the L120 and L160 simulations, we provide two sets of eight lightcones from each box. The electronic mock catalogs are stored as binary data tables conforming to the FITS standard. They consist of a set of rows, one for each galaxy, with information stored in columns with the headings below. In all cases, a missing value is indicated by the value -999 .

- **OBJNO**: A unique identification number for each object (galaxy or star).
- **RA**: Right Ascension.
- **DEC**: Declination.
- **Z**: Redshift (including the peculiar-velocity Doppler shift).
- **MAGR**: The apparent R-band magnitude m_R .
- **ABSBMAG**: The absolute B-band magnitude M_B .
- **UB_0**: The rest-frame $U - B$ color.
- **ZQUALITY**: Analogous to the DEEP2 redshift-quality flag Q , except that we do not use all of the the DEEP2 confidence codes from $Q=1$ to 4. Galaxies that are assigned successful redshifts in our mock-observation algorithms have $Q = 4$, targeted galaxies that had redshift failures in our algorithm have $Q = 1$, stars have $Q = -1$, and galaxies not targeted for spectroscopy have $Q = -2$.
- **SELECTED**: Galaxies that passed the redshift selection cut in Equation 10 (or the weighted redshift selection we apply in the EGS mocks) have this field set to unity.
- **MASKREGION** Galaxies that fall in the region used for DEEP2 maskmaking, rather than the buffer region around the edge, have this field set to unity. Limiting to these galaxies and the ones flagged in the previous item is important for estimating the DEEP2 selection function in many cases.

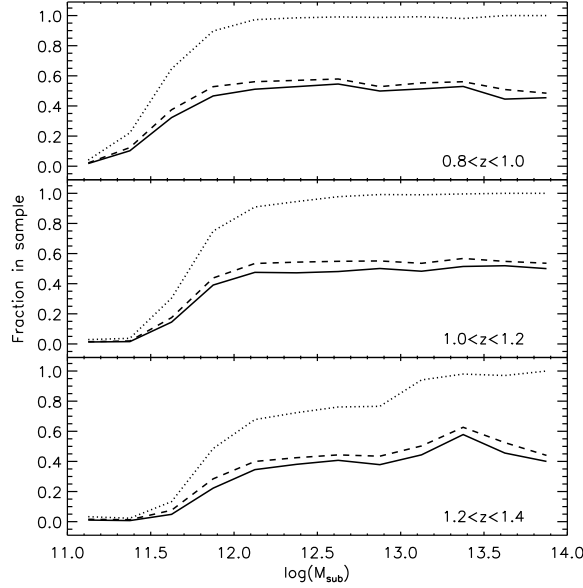


Figure 13. The selection function of mock DEEP2 galaxies versus subhalo mass, in bins of redshift. Solid lines show the fraction of subhalos that contain a galaxy that was included in the sample of observed mock galaxies with successful redshifts in the mocks. Dashed lines show the fraction that were scheduled for observation by the DEEP2 spectroscopic targeting algorithm. Dotted lines show the fraction that exceed the DEEP2 $R = 24.1$ apparent magnitude limit.

- **PGAL** Analogous to the DEEP2 star-galaxy separation probability. Mock galaxies have this field set to unity; stars have it set to zero.
- **XPOS**, **YPOS**, and **ZPOS** The xyz position of this galaxy in the simulation box (in units of the box size).
- **VR** The velocity of this galaxy along the line of sight (where positive velocity implies movement away from the observer). This can be combined with the Z value to compute the cosmological redshift.
- **GROUPID** A unique identifier for the distinct (parent) halo to which this galaxy belongs.
- **HALOID** A unique identifier for the subhalo to which this galaxy belongs.
- **MASS**¹⁵ The virial mass of this galaxy’s dark-matter subhalo, as defined in Bryan & Norman (1998).
- **VMAX** The maximum circular velocity of the subhalo (at the present time).
- **GROUPMASS** The mass of this galaxy’s parent halo
- **CENTRAL** Galaxies that are the central galaxies of their parent halos have this field set to unity.
- **SIGMA7_RAW** Seventh-nearest neighbor surface density Σ_7 for this galaxy, computed before applying DEEP2 selection cuts.
- **DELTA7_RAW** Seventh-nearest neighbor overdensity $\delta_7 = \Sigma_7 / \langle \Sigma_7(z) \rangle$
- **SIGMA3_OBS** Third-nearest neighbor surface density Σ_3 for this galaxy, computed after applying DEEP2 selection cuts.
- **DELTA3_OBS** Third-nearest neighbor overdensity $\delta_3 = \Sigma_3 / \langle \Sigma_3(z) \rangle$.
- **ECOMDIST** Comoving distance to the edge of the survey in comoving h^{-1} Mpc. If this value is less than $1h^{-1}$ Mpc, the value of δ_3 for this galaxy is likely to be inaccurate.
- **EANGDIST** Angular distance to the edge of the survey. (This column and the previous one are only defined for observed galaxies.)
- **WEIGHT** The incompleteness weight w_{corr} assigned to this galaxy.

¹⁵ This column is named **M180** in the L120 and L160 mocks, where it gives the mass computed within a sphere whose radius

is that at which the subhalo density is 180 times the background density.

The mass dependence of DEEP2 selection

One of our goals in producing mock catalogs was to understand the selection probability of DEEP2 galaxies as a function of their halo mass. As we discussed in Sections 3.2.2, the overall mass-selection function in the mocks is likely to have a low-mass cutoff that is sharper than is the case in the real universe, owing to the zero-scatter abundance matching model we used to populate the N-body model with galaxies; however, it is possible that other mass-dependent selection effects will dominate, making the precise shape of the HOD cutoff less relevant. At any rate, because various DEEP2 selection effects, including targeting and redshift-failure effects, depend on local galaxy density, color, and apparent magnitude, one may well be concerned that the DEEP2 selection function might be a strong function of halo mass, beyond the cutoff at low mass from the magnitude limit. We can investigate this in detail with the mock catalogs produced in this study.

Figure 13 shows the fraction of mock galaxies that passed various DEEP2 selection cuts, in three different redshift ranges, as a function of subhalo mass. Dotted lines show galaxies with $R \leq 24.1$, dashed lines show galaxies that were assigned to spectroscopic slits by the slitmask-making algorithm, and solid lines show galaxies that were successfully assigned redshifts. To produce these curves, we selected galaxies with `SELECTED`, `MASKREGION`, and `PGAL` values equal to unity (to exclude galaxies that had no probability of selection); then we computed the fraction that had `MAGR` ≤ 24.1 and `ZQUALITY` greater than zero and equal to 4, respectively. The figure shows a broad mass cutoff in the mocks, spanning nearly an order of magnitude in mass at $z \sim 1$. The breadth of this transition occurs mostly because the DEEP2 flux limit translates into a strongly color-dependent luminosity cut, as shown in Figure 8. This transition is probably somewhat broader in reality, since the mock HOD cuts off too sharply at low masses; however, the dominant effect is the variable absolute magnitude limit, not the shape of the HOD, since the cutoff in the HOD (*cf.* Figure 12) is sharper than the cutoff in mass shown in Figure 13.

The mass cutoff also broadens further at higher redshift, such that the magnitude limit alone introduces some level of incompleteness all the way up to $M \sim 10^{13.5}$, the mass scale of massive groups, at the highest redshifts in DEEP2. It is important to note, though, that this figure considers only the detection probability of the single galaxy at the center of each halo or subhalo. Massive group and cluster halos, containing multiple galaxies, might still have their satellites detected, even if their centrals are not, so the selection function for groups will look somewhat different than this (Gerke et al. 2012).

The mass dependence of the DEEP2 targeting and redshift failures is much weaker than the magnitude selection. There is a slight drop in the spectroscopic targeting rate at high masses, particularly at high redshift. This can probably be attributed to the crowding of slits on DEIMOS slitmasks, which will be somewhat more severe for galaxies in groups and clusters. However, as discussed in several other papers (Cooper et al. 2005; Gerke et al. 2005, 2012), such crowding effects on the sky do not necessarily translate into strong selection effects in three-space; hence, the impact on the mass-selection function here is quite weak. There is also a slight increase in the redshift-success rate with mass, corresponding to the drop in redshift success for the faintest apparent magnitudes. However, the main conclusion from this figure is that, for most applications, the targeting and redshift-failure rates in DEEP2 can safely be approximated as flat functions of mass.